Journal of Microwave Power and Electromagnetic Energy

Numerical Modeling of Microwave Heating of A Porous Catalyst Bed

--Manuscript Draft--

Manuscript Number:	TPEE-2018-0022
Article Type:	Research Article
Full Title:	Numerical Modeling of Microwave Heating of A Porous Catalyst Bed
Keywords:	multiphysics modeling, catalytic upgrading lignin, pyrolysis, porous media
Order of Authors:	Pranjali D Muley, PhD
	Krishnaswamy Nandakumar, PhD
	Dorin Boldor
Abstract:	A Multiphysics numerical model was developed using COMSOL Multiphysics to study the effect of size, shape and position of catalyst bed within the microwave reactor (2450 MHz). The dielectric properties of HZSM-5 catalyst were measured at different frequencies and nine different temperatures ranging from 250° - 700°K. The heat transfer in porous media was coupled with RF electromagnetics module and flow through porous media by extracting the heat source term Q for the heat transfer problem from the electromagnetics. A solid-fluid thermal non-equilibrium condition was modeled as the heat is generated within the catalyst. It was observed that sample position, shape and size of the sample, all significantly affect the heating profile and temperature gradient inside the porous media. The experimental results and the predicted temperatures were in good agreement. Microwave heating had higher total internal energy but conventional heating had lower temperature gradient after reaching steady state. Brick shaped sample heats more uniformly compared to cylindrical sample. If the radius of the sample is decreased, while maintaining the volume of the sample, microwaves penetrate deeper inside the sample, and more uniform temperature distribution is observed throughout the length of sample.

Numerical Modeling of Microwave Heating of A Porous Catalyst Bed

ABSTRACT

A Multiphysics numerical model was developed using COMSOL Multiphysics to study the effect of size, shape and position of catalyst bed within the microwave reactor (2450 MHz). The dielectric properties of HZSM-5 catalyst were measured at different frequencies and nine different temperatures ranging from 250° - 700°K. The heat transfer in porous media was coupled with RF electromagnetics module and flow through porous media by extracting the heat source term Q for the heat transfer problem from the electromagnetics. A solid-fluid thermal non-equilibrium condition was modeled as the heat is generated within the catalyst. It was observed that sample position, shape and size of the sample, all significantly affect the heating profile and temperature gradient inside the porous media. The experimental results and the predicted temperatures were in good agreement. Microwave heating had higher total internal energy but conventional heating had lower temperature gradient after reaching steady state. Brick shaped sample heats more uniformly compared to cylindrical sample. If the radius of the sample is decreased, while maintaining the volume of the sample, microwaves penetrate deeper inside the sample, and more uniform temperature distribution is observed throughout the length of sample.

KEYWORDS: multiphysics modeling, catalytic upgrading lignin, pyrolysis, porous media

1. INTRODUCTION

Thermo-catalytic treatments of bio-oil from biomass pyrolysis (including lignin) have shown to improve biofuel quality (Muley P. D. et al. 2016). Thus, it is important to develop an efficient catalytic heating mechanism that maximizes the energy transfer. There are numerous drawbacks for conventional heating of catalyst bed reactors; amongst the most limiting one is the temperature gradient in radial heat transfer of packed bed reactors (Muley Pranjali D. et al. 2015). Since most conventional reactors are designed to provide heat at the outer region of the reactor tube, most of the energy is rapidly consumed by the outer layers of the packed bed, affecting the rate of reaction in the inner layers. This type of heat profile is especially unsuitable for upgrading of pyrolysis vapors, as the incoming vapors tend to condense on the relatively cooler catalyst area at the center of the reactor which causes catalyst fouling and a marked decrease in yield and quality of bio-oil (Muley P. D. et al. 2016). Moreover, the catalyst on the outer tubular region may heat to very high temperatures which cause the pyrolysis vapors to break down to incondensable gases (CO, CO_2, H_2, CH_4 etc.) rather than a condensable bio-oil that can be used in liquid form (Muley P. D. et al. 2016). In spite of improved heat- transfer designs, conventional heating technology lacks efficient and optimum use of imparted energy to achieve the desired uniform temperature distribution.

Microwave heating, on the other hand, induces heat at the molecular level by directly converting the electromagnetic field into heat, resulting in a temperature gradient, where the core temperature can be greater than the surface temperature (Fernández). These properties of microwave heating make it a more efficient heating method compared to conventional heating, with a conversion efficiency of electrical energy to heat that can reach 80%-85% (Lam and Chase 2012). Although there are few mechanisms that could explain the dielectric response to electromagnetic field, dipolar polarization and ionic conduction dominate at the microwave frequencies. Both these responses depend on the dielectric properties of the material (i.e. dielectric permittivity) and hold especially true for liquids, semi-solids and gases. For dry or partially dry solids without dipoles such as zeolites and carbon-based materials (commonly used as porous catalysts), the theory of dipolar rotation and ionic conduction does not entirely explain the microwave heating mechanism.

It has been proposed that in certain materials such as carbon, some charged particles (electrons) are free to move but only in a delimited region of the material. In this region, a current is induced which produces similar effect as that of ionic conduction in liquids, gases and other ionic mixtures. In the constricted region of the material, the charged particles vibrate, dissipating electromagnetic energy as heat via what is known as the Maxwell-Wagner effect (Menéndez et al. 2010). In other materials such as zeolites, the microwave heating mechanism is not extensively studied. Among the existing studies, an important one was conducted on microwave heating of zeolites which explains the heating mechanism as an ionic rattling effect within the zeolite structure (Komarneni and Roy 1986). According to another study conducted by Ohgushi et al., when hydrated zeolites were irradiated by microwaves, they initially heat due to the moisture present. Once the adsorbed moisture is completely desorbed, the dry zeolite continues to heats directly due to their lossy dielectric nature up to 500 *°C,* at which point thermal runaway occurs (Ohgushi et al. 2001).

The relation between permittivity ε (which dictates the behavior of an electromagnetic field) and dielectric constant ε' and dielectric loss factor ε'' is given by the complex equation (Gabriel et al. 1998):

$$\varepsilon = \varepsilon' - j\varepsilon'' \qquad [1]$$

Where real part (or dielectric constant) ε' is defined as the ability of the material to store imparted microwave energy and the imaginary part (or the dielectric loss factor) ε'' stands for the ability of material to convert the electromagnetic energy into heat.

Operational parameters such as microwave frequency and system's geometry, and material properties such as viscosity, density, temperature, molecular weight, concentration etc. also affect the response of material to microwave field especially those that are temperature dependent. Dielectric properties play an important role in calculating energy efficiency of the reaction process. The amount of energy absorbed and dissipated as heat can be given as (Nelson 1992):

$$P_{abs} = \sigma E^2 = 2\pi f \varepsilon_0 \varepsilon'' E^2 \qquad [2]$$

Where, P_{abs} is volumetric power absorbed (*W/m³*), σ is the conductivity (*S/m*), f is frequency (*Hz*), ε_0 is the dielectric constant of the vacuum, ε'' is relative dielectric loss, E is electric field intensity (*V/m*).

Apart from increased heating efficiency, microwave heating of catalyst may improve catalyst performance compared to conventional heating. There are several reports in literature documenting the increased rate of reaction with the use of microwave heating (Terigar et al. 2010),(Inoue et al. 2002), (Lidstrom et al. 2001).

Due to the aforementioned potential advantages of microwave technology applied to chemistry, the technology is now extensively studied to investigate the effect of microwave heating of catalysts in endothermic reactions. Perry et al., [13] studied the effect of microwave heating of catalyst in methanol steam reforming reaction using both experimental and numerical methods (Perry et al. 2002). They developed a 1D heat transfer numerical model in a single pellet and a 2-D model for heat transfer in packed bed tubular reactor, and the experimental results validated the proposed model. Both 1D pellet model and the 2-D tubular reactor model showed elimination of radial heat transfer effects, space gradient and hot spot formation, confirming that improved performance of the catalyst in experiments was related to its more uniform heating. Other microwave heating studies report improvement in catalyst performance for heterogeneously catalyzed reactions such as conversion of methane (Ioffe et al. 1995), catalytic oxygenation of benzene (Zhang et al. 2012) attributed to better catalytic activity and improved oxidation efficiency due to dipolar polarization effects and stable bed temperatures.

In order to design an experimental set up for microwave heating of catalyst for pyrolysis vapor upgrading, it is important to understand how the catalyst can be heated in the given microwave cavity. Operational parameters such as penetration depth of the material, frequency of microwave, geometry of reactor and material properties are important parameters to be considered for the design of microwave reactors (Cablewski et al. 1994). A numerical analysis can be employed to understand the effects of these parameters on the process and provide guidance for further experimental studies. Numerous numerical studies have been conducted to study microwave heating of porous media, with most of them representing food industry applications. Rakesh et al., conducted a study to understand the temporal and spatial temperature and moisture patterns in food cooked in a combination of microwaves and hot air (Datta 2008). Nicolas et al., studied the heat and mass transfer in bread baking using COMSOL multiphysics (V. Nicolas et al. 2010). For the non-food industry related applications, Chen et al., numerically studied the effect of microwave power on catalyst bed heating and methane decomposition reaction (Chen et al. 2013).

The objective of this study was to numerically investigate the microwave and conventional heating of a porous catalyst bed in order to understand the heat and flow profiles within the reactor. The effect of size, shape and position of catalyst bed inside the microwave on the temperature attained and the overall heating profile was investigated. To our knowledge, this is the first study reporting an in depth sensitivity analysis of the effect of microwave heating in a continuous flow system for catalytic upgrading of pyrolysis bio-oil that accounts for the multiple interactions between Maxwell's equations governing EM heating, heat transfer, and flow through porous media while considering temperature dependent dielectric properties and variable configurations.

2. MODEL DEVELOPMENT

COMSOL 5.1 multiphysics software [COMSOL Inc. Boston, MA, USA] was used to solve the numerical problem with temperature dependent properties. The heat transfer and flow through porous media was coupled with RF electromagnetics module by extracting the heat source term Q for the heat transfer problem from the electromagnetics.

2.1 *Governing Equations*

<u>*Electromagnetics*</u>

The governing equation for electromagnetic wave propagation in a medium is given by Maxwell's equations (Muley Pranjali D. and Boldor 2012)

$$\nabla \cdot \vec{D} = \rho \qquad [3]$$

$$\nabla \times \vec{E} = -\frac{\partial \vec{B}}{\partial t} \qquad [4]$$

$$\nabla \cdot \vec{B} = 0 \qquad [5]$$

$$\nabla \times \vec{H} = \vec{J} + \frac{\partial \vec{D}}{\partial t} \qquad [6]$$

$$\vec{D} = \varepsilon' \varepsilon_0 \vec{E} \qquad [7]$$

$$\vec{B} = \mu' \mu_0 \vec{H} \qquad [8]$$

$$\vec{J} = \sigma_e \vec{E} \qquad [9]$$

where, E is the electric field; B is the magnetic flux density; ρ is electric charge density; J is the electric current; σ_e is electrical conductivity; D is electric displacement; ε_0 is the permittivity of free space $(8.854x10^{-12})$ F/m; H is magnetic field intensity; ε' is the relative dielectric constant; t is time (s); μ' is relative permeability of material; μ_0 is magnetic permeability of vacuum $(4\pi\ x\ 10^{-7})\ N/A^2$

To determine the electric field distribution in a TE_{10} rectangular waveguide (used as a microwave cavity), a wave equation derived from Maxwell's equations is solved (Muley Pranjali D. and Boldor 2012),

$$\nabla \times \left(\frac{1}{\mu'}\nabla \times \vec{E}\right) - \frac{\omega^2}{c}(\varepsilon' - j\varepsilon")\vec{E} = 0 \qquad [10]$$

Total volumetric power generation due to microwave is calculated by the following equation (Muley Pranjali D. and Boldor 2012)

$$Q_{gen} = \sigma_e E^2 = 2\pi f \varepsilon_0 \varepsilon'' {E_{rms}}^2 \qquad [11]$$

Q_{gen} is power absorbed from microwave, which is used as a heat generation term in Fourier equation (W/m^3), σ_e is the conductivity (S/m), f is the frequency (Hz).

<u>*Heat transfer*</u>

The source of heat was direct heating of catalyst bed due to electromagnetic heating. Generally, heat transfer in porous media is given by the following equation (Muley Pranjali D. and Boldor 2012)

$$(\rho C_p)_{eq}\frac{\delta T}{\delta t} + \rho C_p u \cdot \nabla T = \nabla \cdot \left(k_{eq}\nabla T\right) + Q_{gen} \qquad [12]$$

Where ρ and C_p are the fluid density and heat capacity of the fluid, whereas $(\rho C_p)_{eq}$ is defined as the equivalent volumetric heat capacity at constant pressure. k_{eq} is the equivalent thermal conductivity, u is defined as the Darcy's velocity expressed as volume flow rate per unit cross sectional area; Q_{gen} is the heat source. The equivalent terms are related to the respective property of the solid and the fluid. Thus, k_{eq} is the equivalent solid-fluid conductivity given by (Multiphysics 2015),

$$k_{eq} = \theta_s k_s + \theta_L k \qquad [13]$$

And the volumetric heat capacity for solid-fluid system is given by (Multiphysics 2015),

$$(\rho C_p)_{eq} = \theta_s \rho_s C_s + \theta_L \rho C_p \qquad [14]$$

Where, $\theta_s + \theta_L = 1$

Where, θ_s and θ_L are volume fractions of solid and fluid (porosity) material respectively. These equations assume local thermal equilibrium within the solid and fluid material within the porous body. However, since the heat is generated within the porous material, this assumption is not valid and the solid and fluid temperatures in the porous domain are not in equilibrium. A local thermal non-equilibrium condition should be defined for the solid and fluid interaction within the porous structure. This is achieved by coupling the heat equations in the solid and fluid subdomains through a transfer term proportional to the temperature difference between the fluid and the solid. The Local Thermal Non-Equilibrium (*LTNE*) Equations are given as follows;

For solid phase (Multiphysics 2015);

$$\theta_s (\rho c_p)_s \frac{\delta T_s}{\delta t} = \theta_s \nabla \cdot (k_s \nabla T_s) + \theta_s q_s + h(T_f - T_s) \qquad [15]$$

For fluid phase (Multiphysics 2015);

$$\theta_L(\rho c_p)_f \frac{\delta T_f}{\delta t} + \left(\rho C_p\right)_f u \cdot \nabla T_f = \theta_L \nabla \cdot \left(k_f \nabla T_f\right) + \theta_L q_f + h(T_s - T_f) \quad [16]$$

Where, ρ is the density, C_p is the heat capacity, k_s and k_f are solid and fluid thermal conductivities, q is the interstitial convective heat transfer coefficient, u is the velocity and h is the heat transfer coefficient. The critical step in solving this equation is the determination of heat transfer coefficient, h. There are numerous studies reported which have established a correlation for appropriate value of h (Bejan 1995; Alazmi and Vafai 1999; Minkowycz et al. 1999; Saito and de Lemos 2005). In general, heat transfer coefficient is given by $h = a_{fs}h^*$, where a_{fs} is the specific surface area given by $a_{fs} = 6(1 - \varphi)/d_p$, and h^* is given as;

$$\frac{1}{h^*} = \frac{d_p}{Nu_{fs}k_f} + \frac{d_p}{\beta k_s} \quad [17]$$

Where d_p is the particle diameter, Nu_{fs} is the fluid to solid Nusselt number, β is 10 for spherical particles, Nusselt number for the solid to fluid interface is dependent on Reynolds number. For $R_e > 100$ an expression for Nusselt number is given by (Handley and Heggs 1968);

$$Nu_{fs} = \left(\frac{0.255}{\varphi}\right) P_r^{1/3} Re_p^{2/3} \quad [18]$$

This equation is valid for catalyst bed packing of various shapes including spherical, cylindrical and plate shaped packings (Handley and Heggs 1968). In our method, the COMSOL multiphysics software evaluates the Reynolds number based on the velocity in the porous region. There are various other parameters that affect the heat transfer between solid and fluid in the porous region, such as the effect of turbulent and transient flows, variable porosity, thermal dispersion as well as the effects of pressure and viscous dissipation. These additional effects were not considered in the present study. The heat transfer in open regions was solved using regular conduction convection equations as applicable.

Free and porous media flow

The flow of gases through the free and porous region of the tube was solved. The flow of gases through open regions in described by Navier-Stokes equation (Multiphysics 2015)

$$\rho_m \left(\frac{\partial_u}{\partial_t} + u \cdot \nabla u\right) = -\nabla P + \mu \nabla^2 u + F \qquad [19]$$

Continuity equation is (Multiphysics 2015)

$$\nabla \cdot \vec{u} = 0$$

Where; u is velocity of fluid in (*m/s*); μ is viscosity in ($P_a \cdot s$); P is pressure (*Pa*); F is other forces such as gravity or centrifugal force per unit volume (N/m^3)

Whereas, Brinkman equation is used to describe the flow of gases through porous matrix and is given by (Multiphysics 2015);

$$\frac{\rho}{\varepsilon_p}\left(\frac{du}{dt} + (u \cdot \nabla)\frac{u}{\varepsilon_p}\right) = \left[-\nabla \mathrm{P} + \frac{\mu}{\varepsilon_p}\nabla^2 u - \frac{2\mu}{3\varepsilon_p}\nabla^2 u\right] - \left(\mu k^{-1} u + \beta_F |u|^2 + \frac{Q_{br}}{\varepsilon_p^2} u\right) + F \quad [20]$$

$$\rho \nabla \cdot u = Q_{br}$$

Where, ε_p is the porosity, k is the relative permeability, β is the effective viscosity and Q_{br} is the total discharge.

2.2 *Assumptions*

High frequency electromagnetism module was coupled with heat transfer in porous medium and flow through porous media using COMSOL Multiphysics 5.1. To reduce the complexity of the model, certain assumptions were made for the model development.

- The porous media was considered uniformly porous throughout the catalyst bed.
- Thermal properties were constant with changing temperature
- No chemical reaction or phase change occurred.

- Quartz tube with the catalyst bed placed inside the microwave was completely transparent to the microwaves.
- Waveguide walls are perfect conductors with no absorption of microwave energy by the cavity or air.
- Average inlet velocity was *0.125 m/s* as measured during experimental validation runs

2.3 *Geometry*

A *3-D* geometry of a pilot scale microwave waveguide was built in COMSOL 5.1 (**Figure 1**). The setup consisted of a 1.2 kW, 2450 MHz power source, connected to an aluminum waveguide of dimensions *1.37 m* long, *0.106 m* wide and *0.053 m* deep (Industrial Microwave Systems (IMS), Inc. Morrisville, NC), shorted at the far end. The porous catalyst bed was placed inside a quartz tube with *0.014 m* internal radius and *0.49 m* length sitting at the center of the waveguide. The catalyst bed has a *0.014 m* radius and is *0.15 m* long initially placed at the center of the quartz tube.

2.4 *Boundary conditions*

Electromagnetic Waves

The microwave power was set at *400 W* for all combinations investigated. The electromagnetics wave module was active in all domains. The microwave energy was supplied to the cavity through the rectangular waveguide at port one in TE_{10} mode electric. The dielectric properties of the catalyst bed were measured as described in section 3.1 and defined in the model, the dielectric properties were temperature dependent and given by equation $0.065*\exp(-0.002*T)$(where T is temperature in °C). Scattering boundary conditions were defined at the outlet and inlet of the quartz tube in order to avoid undesired reflections and perturbations in the field caused by sudden discontinuity in the waveguide. A continuity boundary condition was applied to all the internal boundaries of the domains.

Heat Transfer in Porous Media

Heat transfer in porous media module was coupled with the electromagnetics and flow module. The porous matrix was the catalyst bed whose porosity was measured in lab to be 0.67. The density (*720* kg/m^{3}), thermal conductivity (*0.12* W/m^2K) and specific heat (*1369 J/kg °K*) of the material were obtained for material properties from Zeolyst International. The heat source Q_{gen} was set as the electromagnetic power loss density calculated from electromagnetics module. Convective cooling was defined for the outer walls of the waveguide and quartz tube walls. Conjugate heat transfer was active in all domains.

Free and Porous Media Flow

The laminar flow module was active in the quartz tube only. The inlet velocity of the fluid was measured as *0.125 m/s,* and the inlet temperature was *150 °C*. The porosity was determined to be *0.67* and was assumed to be uniform throughout the catalyst bed.

2.5 *Mesh Generation*

The element size requirement for solving the electromagnetic problem is that the maximum grid element size (S_{max}) should be less than half the wavelength. This requirement is known as the Nyquist criterion and is defined as,

$$S_{max} < \frac{\lambda}{2} = \frac{c}{2f\sqrt{\varepsilon'\mu'}} \qquad [23]$$

Where, λ is the wavelength (*m*), f is the frequency (*Hz*), c is the speed of light in vacuum (*m/s*), ε' is the relative dielectric constant, and μ' is the relative permeability. Based on this criterion, the default fine mesh size was used where the maximum element size was set conservatively at 0.00614 *m* in the waveguide and the maximum element size was set to *0.00116 m* for quartz tube and porous media. The models were tested at 3 different mesh sizes of (cavity element number, reaction tube element number) = (243599, 32229), (306159, 41004), (490640, 81895) and the grid independence for both microwave and conventional heating models was established (**Figure 2**)

The distribution of temperature along the centerline of the catalyst bed in *x* direction is plotted in **Figure 2**. The difference in temperature distribution between all three grid sizes is low, but it is especially negligible between the second (306159, 41003) and third grid size (490640, 81895) and satisfies the grid independence. Thus, further studies were conducted at (490640, 81895) grid size.

2.6 *Solver used*

The frequency domain was used to solve the wave equation in the radio frequency module. The frequency was set to *2.45 GHz*, which is the operating frequency of the microwave. The stationary solver was used to solve heat transfer and fluid flow equations in porous media to obtain the temperature profiles.

2.7 *Methods*

An initial study was conducted to study the effect of sample size, shape and position inside the microwave cavity. A numerical model was developed using COMSOL Multiphysics 5.1 studying the effect of electromagnetic irradiation on porous catalyst bed for this purpose. Gas flow through the porous media was not considered for the preliminary study. The catalyst used is a dielectric material and readily heats up in a microwave reactor. Since the position of catalyst bed inside the reactor plays a crucial role in the uniform heating of catalyst, a sensitivity analysis was performed using five different positions (**Figure 3**);

- center of the waveguide *(z = 0)*
- base of the waveguide ($z=-0.03m$)
- upper edge of the waveguide $z=0.03m$
- $z=-0.01\ m$
- $z=-0.02m$.

The effect of size of the catalyst bed was also tested by designing a smaller diameter tube while maintaining the volume of the catalyst bed. The new design also underwent a sensitivity analysis for 3 different positions; a) center of the waveguide $z=0$, b) $z=-0.01$ and, c) $z=-0.02$. Two shapes of catalyst bed (a) rectangular block and, (b) cylindrical were investigated to study the effect of shape on the temperature profile.

A more thorough secondary study with experimental validation, was performed where the flow of gas through the quartz tube was taken into account. The conjugate heat transfer equation was solved for porous domain where the solid and fluid temperatures are not in equilibrium. The average velocity of the incoming gas was *0.125 m/s* to correspond with the existing experimental conditions as measured. As measured during experimental runs, the incoming gas temperature was *150 °C* and external atmospheric temperature was *25 °C*. A conventional heating model was also developed for comparison. Experimental temperatures at three locations were also measured for model validation. Due to limitations with temperature measurements within the microwave cavity, only three locations were chosen for temperature measurement using IR pyrosensors and thermal camera. The IR sensors were calibrated for quartz glass transparency and emissivity.

3. RESULTS AND DISCUSSION

3.1 *Dielectric properties of HZSM-5 catalyst at different temperatures*

The dielectric properties play an important role in the microwave heating of material. Knowledge of dielectric properties of material under treatment gives a clear understanding of how a particular material will heat under the influence of electromagnetic waves. Depending on the material, dielectric properties may be temperature and frequency dependent.

The dielectric properties of HZSM-5 powder was measured using an Agilent ENA series E5071C Network Analyzer and Agilent 85070E dielectric probe kit (Agilent Technologies, Inc. Santa Carla, CA) using a slim form open-ended probe method in a 201-point frequency sweep from *280 MHz* to *4500 MHz*. The network analyzer was controlled by Agilent 85070E dielectric kit software (Agilent Technologies, Inc. Santa Carla, CA) and calibrated using the 3-point method (short-circuit, air and water at *25 °C*). The NaZSM-5 catalyst was calcined in air at *550 °C* for *5.0 h* to convert NaZSM-5 to HZSM-5. The powder was then filled in a tube surrounded with a heating tape. Dielectric properties were measured at nine different temperatures ranging from *298 ° - 643 °K*.

Figure 3a,b show change in dielectric constant and dielectric loss at different frequencies and different temperatures. While no significant difference was observed with the change in frequency, the dielectric properties were temperature dependent. **Figure 4c,d,e** shows the electrical conductivity, dielectric loss and dielectric constant values at *2450 MHz* frequency for different temperatures. Electric conductivity is given by

$$\sigma = 2\pi f \varepsilon_0 \varepsilon'' \qquad [24]$$

Where, f is frequency (*Hz*), ε_0 is the dielectric constant of the vacuum, $\varepsilon''$is relative dielectric loss of material.

For a material to undergo dielectric heating under microwave radiation, the conductivity of the material should be higher that 0; i.e. the electric field flows through the material. When electric field flows through the material, some of the energy is converted to heat. Materials with $\sigma = 0$ are called lossless material (air, vacuum) and those with very high conductivities ($\sigma >> 0$), are called conductors such as metals. Materials with medium range conductivities ($\sigma > 0$) are called lossy materials and they readily heat in a microwave. Since the conductivity of catalyst is slightly greater than 0, it is categorized as a lossy material (F**igure 4**).

3.2 *Primary Study*

3.2.1 *Effect of position of catalyst bed*

In general, due to the specific propagation of EM waves in the microwave cavities partially filled with a lossy or conductive materials, it is expected that the distribution of the EM field both in the void spaces (air, vacuum) and in the lossy material (load) will be dependent on the specific location and geometry of the load in the cavity. Hence the effect of position of sample on heat profile inside the microwave cavity was investigated. We studied three different locations of dielectric material a.) center of the cavity ($z=0$), b.) base of the waveguide $z=-0.03$ m and, c.) top of the waveguide $z = 0.03$ m. (**Figure 5**)

In case where the dielectric catalyst bed is placed at the center of the cavity (**Figure 5a**), the electric field intensity is observed to decrease as the microwaves travel through the dielectric material. The electric field intensity is lower inside the dielectric material than in the void. The temperature profile is consistent with that of the electric field since microwave heating rate of a dielectric material is proportional to the square of the electric field. Maximum electric field intensity in the catalyst bed was *13561 V/m* and the corresponding temperature was *472 ºC* (**Figure 5a**). It is also observed that most of the energy is absorbed at front end of the catalyst bed located towards the incident wave as expected. Due to the skin-depth effect, as the thickness of the sample increases, current density decreases, resulting in temperature decay along the wave propagation direction (Ratanadecho et al. 2002).

When the catalyst bed is moved close to the base of the waveguide by *3 cm*, most of the electric field is concentrated only in the upper region of the catalyst bed, leaving the base of the catalyst bed unheated (**Figure 5b**). Maximum electric field intensity in the catalyst bed was *14000 V/m* in the waveguide and 10000 *V/m* in the catalyst bed, similar to the case when the catalyst bed is placed in the center of the cavity, and the highest corresponding temperature is *654.46 ºC*. For the same incident power, higher temperature is achieved when the bed is close to the base of the waveguide compared to the center because only a fraction of the catalyst is absorbing the energy. Since some of the catalyst material is outside the electric field area, the energy absorbed is limited to the upper part of the catalyst bed (Vadivambal and Jayas 2010). Similar electric field distribution and temperature profile is observed when the catalyst bed is positioned close to the top of the waveguide (*z=0.03m*) (**Figure 5c**). Since most of the energy is concentrated in the lower part of the catalyst bed, the upper catalyst area is not heated. The maximum electric field intensity in the catalyst bed was *9000 V/m* and the corresponding maximum temperature achieved is *684.47 ºC*. These results were in agreement with the literature where Funawatashi and Suzuki (2003) studied the effect of sample position on the electric and temperature fields (Funawatashi and Suzuki 2003). They observed that electric field greatly depends on the position of a dielectric material and consequently affect the heating rate. Rattanadecho et al., (2009) concluded that the rate of heating of dielectric material significantly changes with position of the material in the microwave waveguide (Cha-um et al. 2009). For all three catalyst position, non-uniform temperature profile was observed. Uneven heating in the microwave cavity is a result of two phenomenon; due to standing wave pattern and due to rapid decay of microwaves and uneven exposure of the catalyst mass to the incident microwaves (Cha-um et al. 2009; Vadivambal and Jayas 2010).

Figure 6 shows the temperature profile in YZ direction at the center of the catalyst bed for five different catalyst bed positions. High temperature zone is at the center when the catalyst bed is positioned at the center of the waveguide (**Figure 6b**). However, as the position of the catalyst bed is changed, the hot spot location changes. Moreover, 320 °C temperature was achieved for the center position as opposed to 500 °C when the catalyst bed was either at the top (**Figure 6a**) or bottom (**Figure 6e**) of the waveguide. This could be attributed to the fact that for the bed position closer to the waveguide wall, a significant part of the catalyst bed remains unheated, creating an undesirably large temperature gradient inside the bed.

We also studied the effect on temperature profile when the catalyst bed is moved slightly off center (10 mm and 20 mm off center) (**Figure 6**). For position z= *10 mm* off center, the highest temperature noted was 600 °C (**figure 6c**). This temperature dropped significantly to only 260 °C when the catalyst was moved *20 mm* off center (to a range of 100 – 260 °C). We also observed that the temperature gradient greatly reduces when the catalyst bed position is *20 mm* off from the center (**Figure 6d**). These observations could be attributed to the smaller sample size which causes arbitrary wave reflection resulting in multimode of field pattern (Cha-um et al. 2009). For a closed microwave cavity like the one studied here, the occurrence of standing waves creates uneven heating. Some methods to cancel or minimize the effect of standing waves pattern is to move the sample continuously, change the size of cavity or change the size and/or position of sample within the cavity. Placing the sample 20 mm off center might have minimized this effect, resulting in lower temperature gradient.

3.2.2 *Effect of catalyst bed dimensions*

We studied the effect of sample configuration on microwave heating. The catalyst bed diameter was reduced while keeping its volume constant via increased bed length. The new sample was positioned at three different locations (center – z = 0, 10mm off center *z=-0.01* and 20 mm off center *z=-0.02*) inside the waveguide to test the effect of position. These positions were selected based on the previous results obtained for larger diameter tube (section 3.2.1). Higher temperature was observed at the front end where the microwaves enter the catalyst bed, but this temperature was lower (by as much as half when located at the center of the waveguide) than that observed in the thicker catalyst bed (**Figure 7**).

As opposed to the earlier model with larger diameter catalyst bed, fewer cold regions were observed for the new geometry (**Figure 7**). This can be explained by the fact that since the thickness of the sample decreased and length increased, the microwave absorption was much softer and more evenly distributed along the length of the bed, as opposed to being absorbed all upfront in the thicker catalyst bed. The ratio of penetration depth to the bed diameter changed and microwaves were absorbed along the complete length of the catalyst bed. Thus, non-uniform heating due to rapid decay of microwaves in the incident direction can be controlled by changing the dimensions of the dielectric sample in this particular configuration. A general trend is that as the sample volume increases, the rate of temperature rise decreases. However, if the thickness of the sample is smaller than the penetration depth of the sample, even with larger volume, a higher rate of temperature rise can be obtained (**Figure 9**).

If the penetration depth of the sample is greater than the thickness of the sample, it causes interference to the waves that are reflected from sample-air interface due to the difference in air and sample dielectric properties. This reflection and transmission at the interfaces contribute to a resonance of standing waves inside the porous sample and the electric field distribution does not decays exponentially from the surface, as expected (Muley Pranjali D. and Boldor 2012), eventually decreasing the rate of temperature rise (Cha-um et al. 2009). It is also noted that the temperature distribution was more uniform when the sample was placed 20 mm away from the center (**figure 7**).

3.2.3 *Effect of sample shape*

We studied the effect of having a rectangular brick shaped sample and compared the results with the cylindrical sample of same volume. More uniform heating was observed for bricked shaped sample compared to cylindrical sample. A sharp rise in temperature was observed in the z direction at the center of the sample (**figure 8**). Cylindrical sample showed higher temperature at the center and cooler temperatures zones at the margins, as well as much more variability in the wave incident direction (x-axis). For cylindrical samples, less of the incident microwave energy is absorbed at the surface prior to reaching the center. Hence a higher concentration of microwave energy is focused at the center causing more heating at the core. This is especially true for narrow diameter tubes where the distance travelled through the lossy portion is smaller. These results were in agreement with literature results comparing three different shapes; cylindrical, brick and hexagonal prism. Vilayannur et al., concluded that for a cylindrical shaped sample, the heating is mostly concentrated at the center of the samples as opposed to the corners in case of brick-shaped samples (Vilayannur et al. 1998). While we did not observe higher heating at the corners for brick shaped sample, the temperature distribution was much more uniform with heating taking place at the corners as well as the center of the sample.

3.3 *Experimental validation and comparison to conventional heating*

3.3.1 *Temperature profile*

A thorough secondary study includes the effect of gases flowing through the porous catalyst bed. **Figure 10** shows the temperature profiles for microwave and conventionally heated catalyst bed. The temperature of the fluid entering the quartz tube was *150 °C*. For the conventional heating model, the walls of catalyst bed were maintained at a constant temperature of *370 °C*. The temperature along the x-axis is plotted (**Figure 11**). The temperature at the core of the catalyst bed is higher for microwave heating and lower towards the wall. However, as expected for conventional heating, higher temperature is obtained at the walls of the catalyst bed and the temperature reduces towards the center. Due to the local thermal non-equilibrium condition, the heat is carried by the fluid and the exit temperature of the fluid is higher than the inlet temperature. The highest temperature achieved by microwave heating was *420 °C* towards the side of the catalyst bed exposed to the incident microwaves.

Numerically predicted temperature was compared to the experimental data obtained during microwave bio-oil vapor upgrading runs using pine sawdust as biomass as previously described (Muley P. D. et al. 2016). Temperature was measured at three different locations in the *X*-direction along the quartz tube. An IR thermocouple and a thermal camera were used for temperature measurement. The numerical predictions were a good match (within 5%) with the experimental temperature results (**Figure 11**). Any discrepancies between the numerical model and the measured temperature of the catalyst bed could be mainly due to the assumption of average flow rate in the model. Since, in reality, the flow rate varies over the time as gas is generated within the system during reactions. Moreover, other external factors such as, local super-heating in the microwave, effect of coke deposition and poisoning of catalyst bed was not precisely modeled and could have affected the accuracy of the model.

A steady rise of temperature (as averaged in the *YZ* plane) is observed for both microwave and conventional heating in *X*-direction (**figure 11**). The temperature profile in z-direction shows a wall to wall temperature gradient within the catalyst bed for both microwave and conventional heating (**figure 9**). The temperature gradient is observed to be from the walls towards the center of the catalyst bed for conventional heating, as expected. The microwave temperature gradient is inversed, as also noted and discussed in the section 3.2 on the model without the gas flow. An effect of reaction kinetics should also be modeled for predicting the temperature profiles within the microwave system accurately. The changes in thermal conductivity and other thermodynamic parameters due to formation of new products and intermediates should be accurately modeled for precision.

3.3.2 *Velocity profile*

The flow was modeled across the porous catalyst bed. The gas inlet velocity was *0.125 m/s*. The velocity profile in longitudinal direction (*xz*- direction) was plotted. The velocity profile was consistent with the boundary conditions. The porous bed was defined as uniformly porous and a drop in velocity was observed in this region. A small recirculation region was also observed at the back ends of the geometry where the vertical tubes meet the horizontal tube. The highest velocity obtained was *0.22 m/s* (**figure 12**).

3.3.3 *Effect of tube diameter*

Similar to the no flow conditions, when the diameter of the tube was reduced to *0.02 m* for narrow tube from *0.028 m* for regular tube and the length was increased from *0.25 m* to *0.4 m*, more uniform temperature distribution was observed (**figure 10**). The overall temperature range as lower for the narrow tube (*20 °C* to *284 °C*) compared to that for the bigger diameter shorter tube (*20 °C* to *420 °C*). A temperature plot across *x* axis was plotted for both tubes (**figure 11**). The temperature in the narrow tube increases to *284 °C* in about *0.1 m* of the tube length and remains steady at that temperature for the remainder of the length, whereas a steady increase is observed for the shorter tube.

4. CONCLUSION

A Multiphysics numerical model studying the microwave heating of porous catalyst bed was developed using COMSOL Multiphysics 5.1. The effect of sample shape, size and position on microwave heating of porous catalyst bed was studied. The model was validated against the experimental data. The temperature profiles obtained from microwave heating was compared to that obtained from conventional heating profile. It was observed that sample position, shape and size of the sample, all significantly affect the heating profile and temperature gradient inside the porous media. Samples placed 20mm away from the center heat more uniformly compared to samples placed at the center, higher temperatures are achieved when the sample is placed 10mm away from the center. This is because stronger resonance effects occur due to disorderly wave reflections within the samples. The experimental results and the predicted temperatures were a close match. Microwave heating had higher total internal energy but conventional heating had lower temperature gradient after reaching steady state. This type of numerical modeling can be used to optimize the process parameters and design an efficient process depending on the ease of operation and manufacturing and the cost efficiency.

ACKNOWLEDGEMENT

The authors would like to acknowledge LSU's Department of Chemical Engineering, LSU's Department of Biological and Agricultural Engineering, LSU's Center for Computation and Technology, LSU Agricultural Center, and USDA NIFA Hatch Program [project number

LAB #94146], for their support of this project. Financial support was provided by US NSF CBET (award #1437810), US NSF OIA (award #1632854), and Louisiana Board of Regents (#Louisiana Board of Regents Support Fund (award #LEQSF(2015-17)-ENH-TR-01). Published with the approval of the Director of the Louisiana Agricultural Experiment Station as manuscript #2018-232-31870.

REFERENCES

Alazmi B, Vafai K. 1999. Analysis of Variants Within the Porous Media Transport Models. J Heat Transfer. 122(2):303-326.
Bejan A. 1995. Convection heat transfer. John Wiley & Sons, Incorporated.
Cablewski T, Faux AF, Strauss CR. 1994. Development and application of a continuous microwave reactor for organic synthesis. The J. org. chem. 59(12):3408-3412.
Cha-um W, Rattanadecho P, Pakdee W. 2009. Experimental analysis of microwave heating of dielectric materials using a rectangular wave guide (MODE: TE10) (Case study: Water layer and saturated porous medium). Exp Therm Fluid Sci. 33(3):472-481.
Chen W-H, Liou H-J, Hung C-I. 2013. A numerical approach of interaction of methane thermocatalytic decomposition and microwave irradiation. Int J Hydrogen Energ. 38(30):13260-13271.
Datta VRaAK. 2008. Coupled Electromagnetics- Multiphase Porous Media Model for Microwave Combination Heating. Excerpt from the Proceedings of the COMSOL Conference Boston 2008
Fernández, Yolanda; Arenillas, Ana; Menéndez, J. Ángel. Microwave heating applied to pyrolysis [Book Chapter]. Advances in Induction and Microwave Heating of Mineral and Organic Materials. 31:30.
Funawatashi Y, Suzuki T. 2003. Numerical analysis of microwave heating of a dielectric. Heat Transfer—Asian Research. 32(3):227-236.
Gabriel C, Gabriel S, Grant EH, Halstead BSJ, Mingos DMP. 1998. Dielectric parameters relevant to microwave dielectric heating. Chem Soc Rev. 27(3):213-223.
Handley D, Heggs PJ. 1968. Momentum and Heat Transfer Mechanism in Regular Shaped Packings [Article]. Trans. of the Institution of Chemical Engineers and the Chemical Engineer. 46(9):T251-&. English.
Inoue C, Hagura Y, Ishikawa M, Suzuki K. 2002. The dielectric property of soybean oil in deep-fat frying and the effect of frequency. J Food Sci. 67(3):1126-1129.
Ioffe MS, Pollington SD, Wan JKS. 1995. High-Power Pulsed Radio-frequency and Microwave Catalytic Processes: Selective Production of Acetylene from the Reaction of Methane over Carbon. J Catal. 151(2):349-355.
Komarneni S, Roy R. 1986. Anomalous microwave melting of zeolites. Mater Lett. 4(2):107-110.
Lam SS, Chase HA. 2012. A Review on Waste to Energy Processes Using Microwave Pyrolysis [Article]. Energies (19961073). 5(10):4209-4232.

Lidstrom P, Tierney J, Wathey B, Westman J. 2001. Microwave assisted organic synthesis - a review. Tetrahedron. 57(45):9225-9283.
Menéndez JA, Arenillas A, Fidalgo B, Fernández Y, Zubizarreta L, Calvo EG, Bermúdez JM. 2010. Microwave heating processes involving carbon materials. Fuel Process Technol. 91(1):1-8.
Minkowycz WJ, Haji-Sheikh A, Vafai K. 1999. On departure from local thermal equilibrium in porous media due to a rapidly changing heat source: the Sparrow number. Int J Heat Mass Transfer. 42(18):3373-3385.
Muley PD, Boldor D. 2012. Multiphysics Numerical Modeling of the Continuous Flow Microwave-Assisted Transesterification Process. J Microw Power Electromagn Energy. 46(3):139-162.
Muley PD, Henkel C, Abdollahi KK, Boldor D. 2015. Pyrolysis and Catalytic Upgrading of Pinewood Sawdust Using Induction Heating Reactor. Energy Fuels.
Muley PD, Henkel CE, Aguilar G, Klasson KT, Boldor D. 2016. Ex situ thermo-catalytic upgrading of biomass pyrolysis vapors using a traveling wave microwave reactor. Appl Energ. 183:995-1004.
Multiphysics C. 2015. Reference Manual, Version 5.0. Google Scholar.
Nelson SO. 1992. Correlating Dielectric Properties of Solids and Particulate Samples Through Mixture Relationships Trans ASAE. 35(2):625-629.
Ohgushi T, Komarneni S, Bhalla A. 2001. Mechanism of Microwave Heating of Zeolite A. J Porous Mater. 8(1):23-35. English.
Perry WL, Datye AK, Prinja AK, Brown LF, Katz JD. 2002. Microwave heating of endothermic catalytic reactions: Reforming of methanol. AlChE J. 48(4):820-831.
Ratanadecho P, Aoki K, Akahori M. 2002. A numerical and experimental investigation of the modeling of microwave heating for liquid layers using a rectangular wave guide (effects of natural convection and dielectric properties). Appl Math Model. 26(3):449-472.
Saito MB, de Lemos MJS. 2005. A Correlation for Interfacial Heat Transfer Coefficient for Turbulent Flow Over an Array of Square Rods. J Heat Transfer. 128(5):444-452.
Terigar BG, Balasubramanian S, Lima M, Boldor D. 2010. Transesterification of soybean and rice bran oil with ethanol in a continuous-flow microwave-assisted system: yields, quality, and reaction kinetics. Energy Fuels. 24:6609-6615.
V. Nicolas PS, PG, VJ, LB, JPP. 2010. Modeling Heat and Mass Transfer in Bread during Baking. Excerpt from the Proceedings of the COMSOL Conference 2010 Paris.
Vadivambal R, Jayas DS. 2010. Non-uniform Temperature Distribution During Microwave Heating of Food Materials—A Review. Food Bioprocess Technol. 3(2):161-171. English.
Vilayannur RS, Puri VM, Anantheswaran RC. 1998. Size and Shape Effect on Non-Uniformity of Temperature and Moisture Distributions in Microwave Heated Food Materials: Part I Simulation. J Food Process Eng. 21(3):209-233.
Zhang YC, Bo LL, Wang XH, Liu HN, Zhang H. 2012. Study on catalytic oxidation of benzene by microwave heating. Huan jing ke xue 33(8):2759-2765. chi.

List of Figures

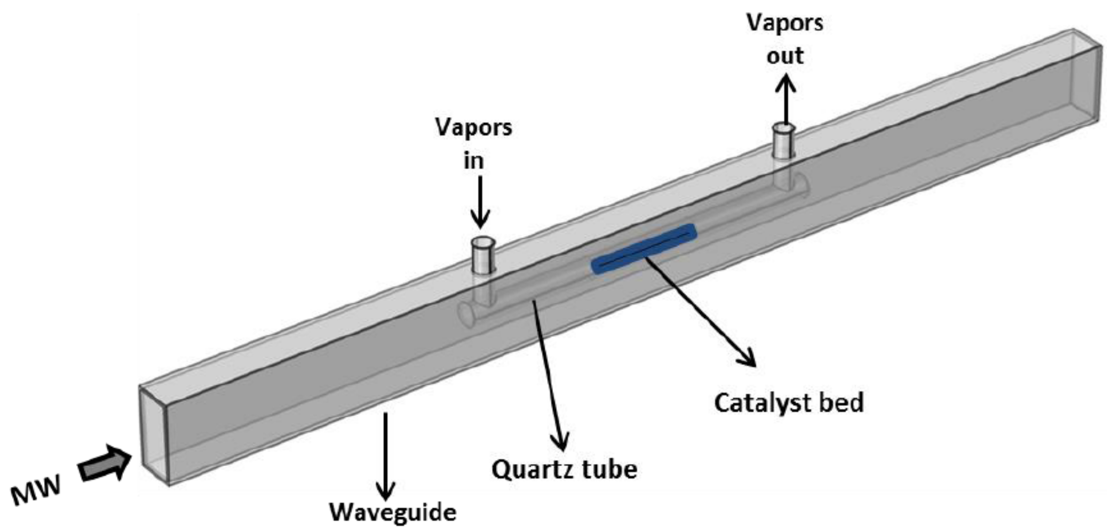

Figure 1 Geometry of microwave system used to heat porous catalyst bed

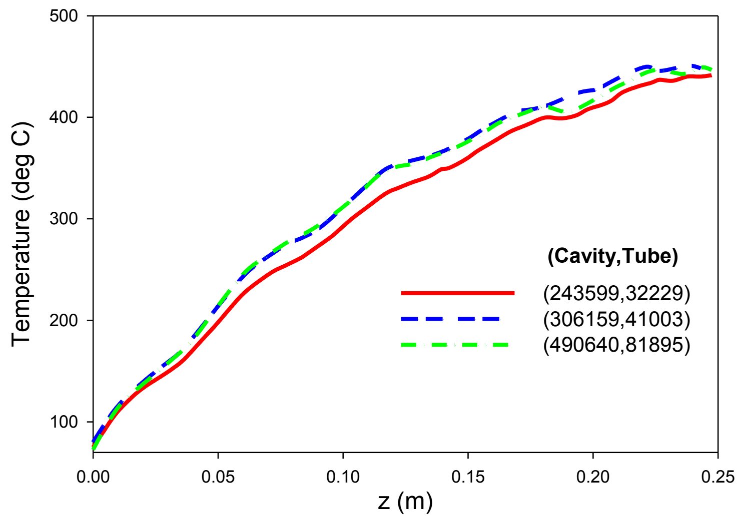

Figure 2 Temperature distributions along the centerline of the reaction tube at three different grid systems

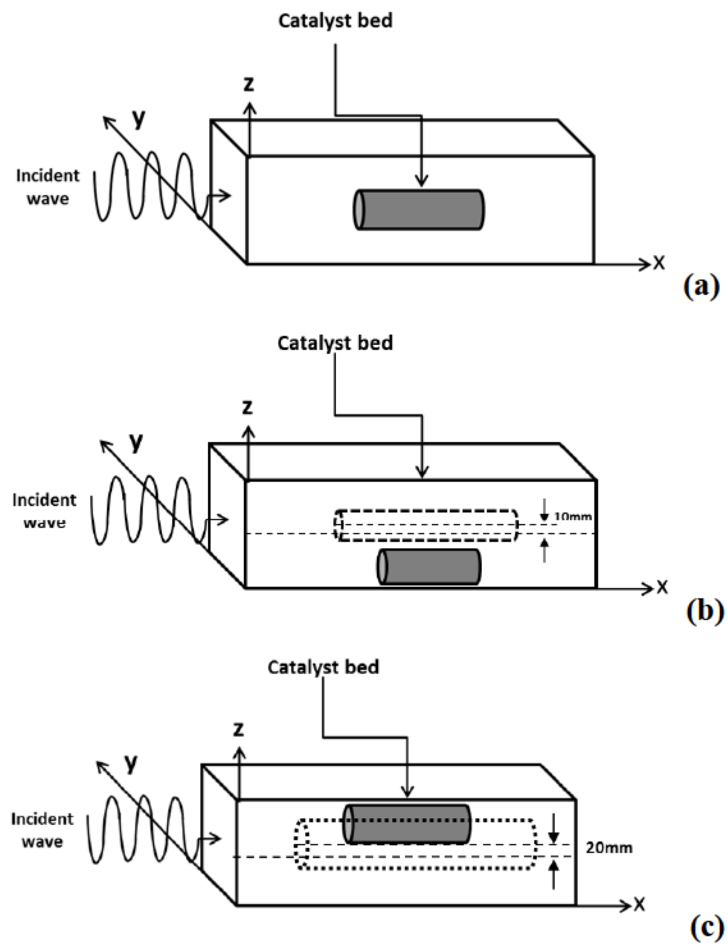

Figure 3 Position of catalyst bed within the waveguide a) center ($z=0$), b) base ($z = -0.03$) (dotted line showing narrow tube *10 mm* away from center), c) top ($z = 0.03$) (dotted line showing narrow tube *20 mm* away from center)

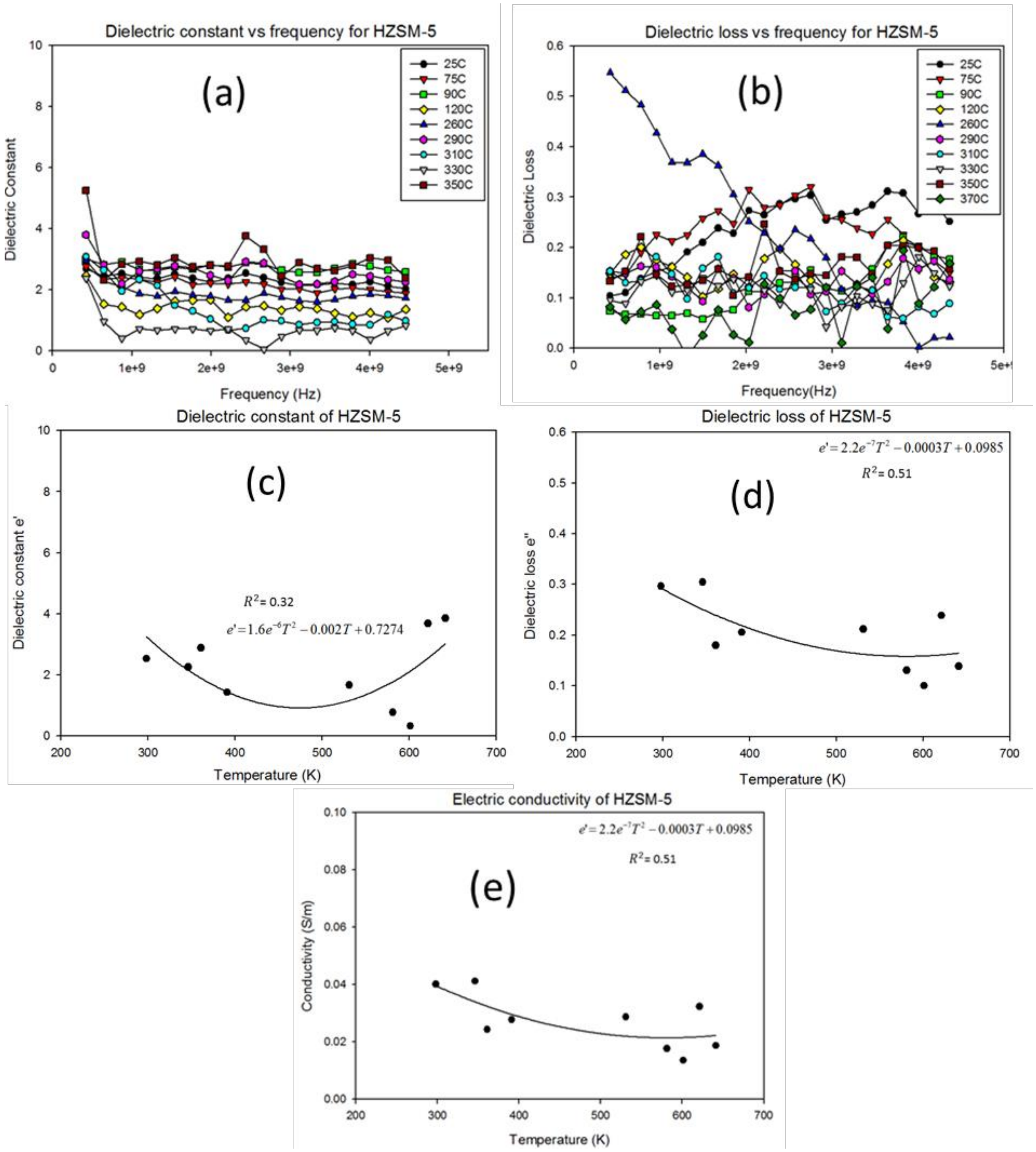

Figure 4 Dielectric properties of HZSM-5 powder at (a) different temperatures and (b) frequencies. (c) Electric conductivity, (d) dielectric loss and (e) dielectric constant of HZSM-5 at *2450 MHz* frequency at varying temperatures

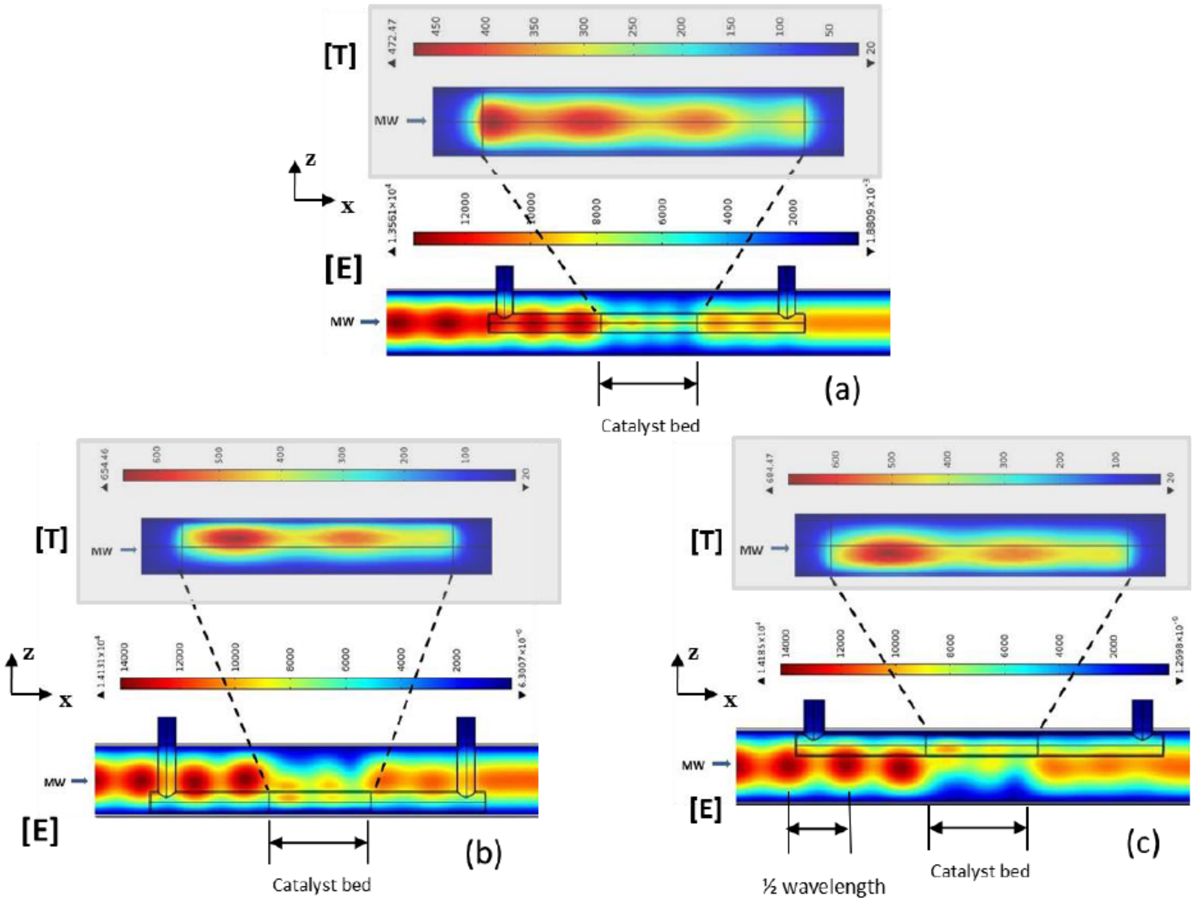

Figure 5 Electric field (V/m) and temperature profile for catalyst bed at (a) the center of the cavity *(z =0), (b)* the base of the cavity *(z =-0.03), (c)* the top of the cavity (*z =0.03*) (Note: different temperature scales)

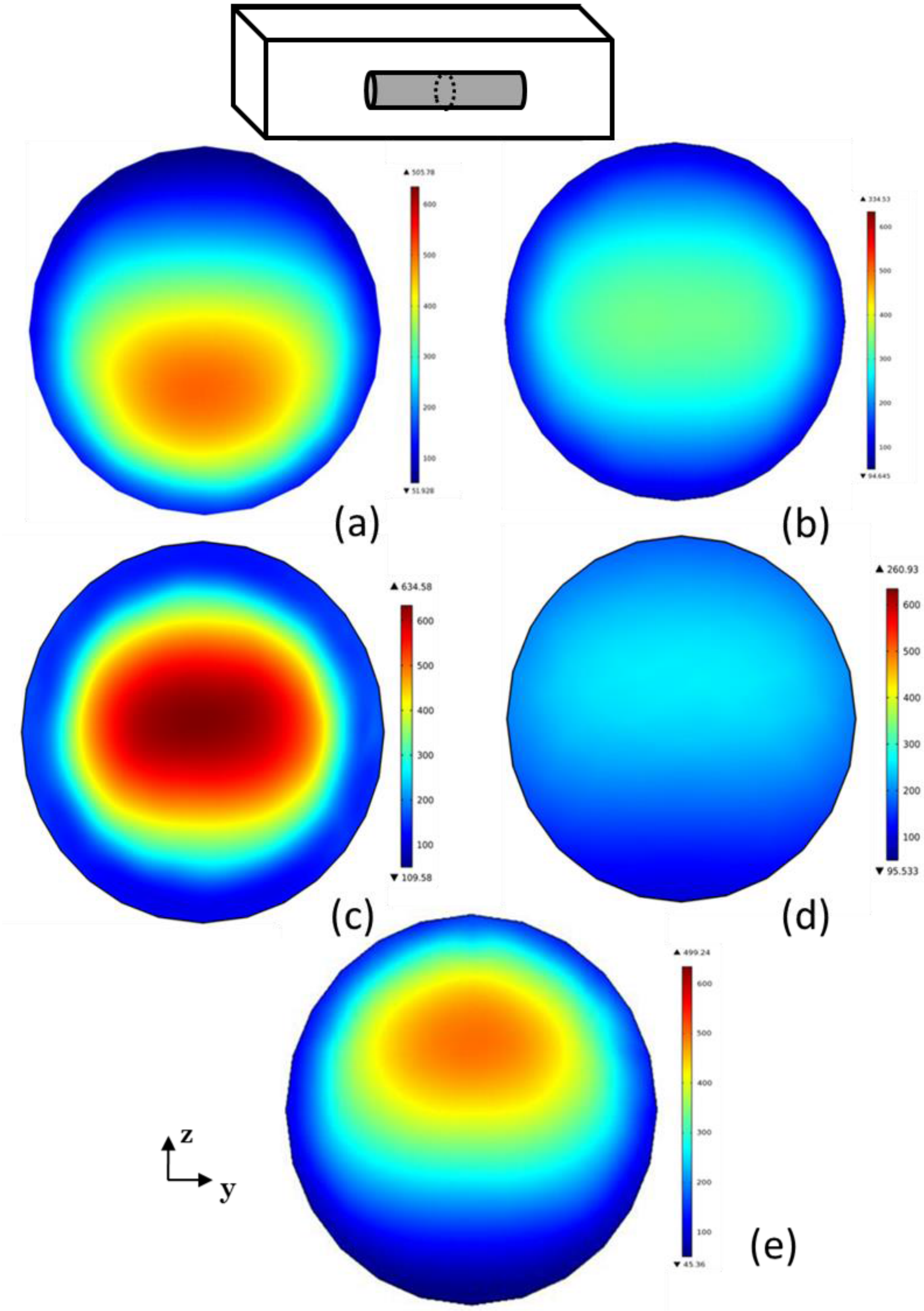

Figure 6 Temperature profile in *YZ*-direction at the center of the catalyst bed. The catalyst bed position is a) top of the waveguide $z=0.03\ m$, b) center of the waveguide $z=0$, c) *10 mm* off from the center $z = -0.01\ m$, d) *20 mm* off from the center of the waveguide $z = -0.02\ m$ and, e) base of the waveguide $z=-0.03\ m$. (Note: different temperature scales)

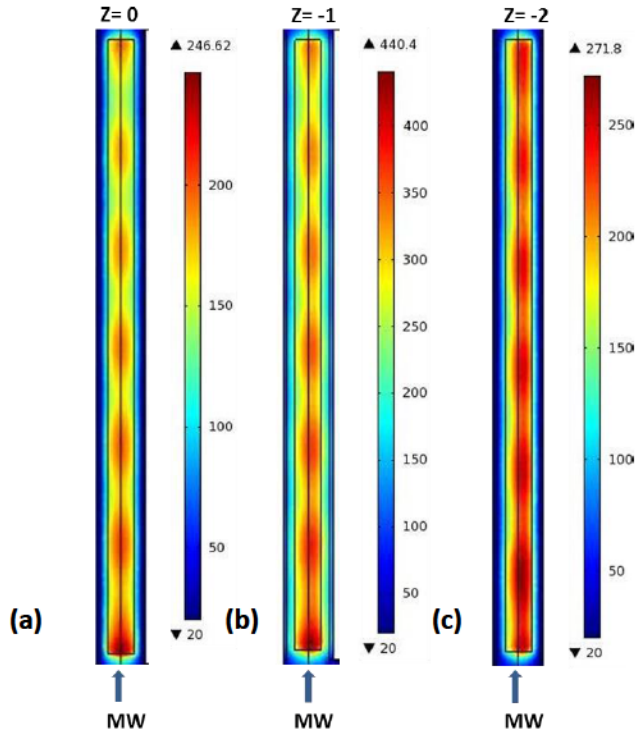

Figure 7 Temperature profile for narrow catalyst bed at different positions a) center (*z=0*), b) *10 mm* away from center (*z=-0.01*) and c) *20 mm* away from center (*z=-0.02*) (Note: different temperature scales)

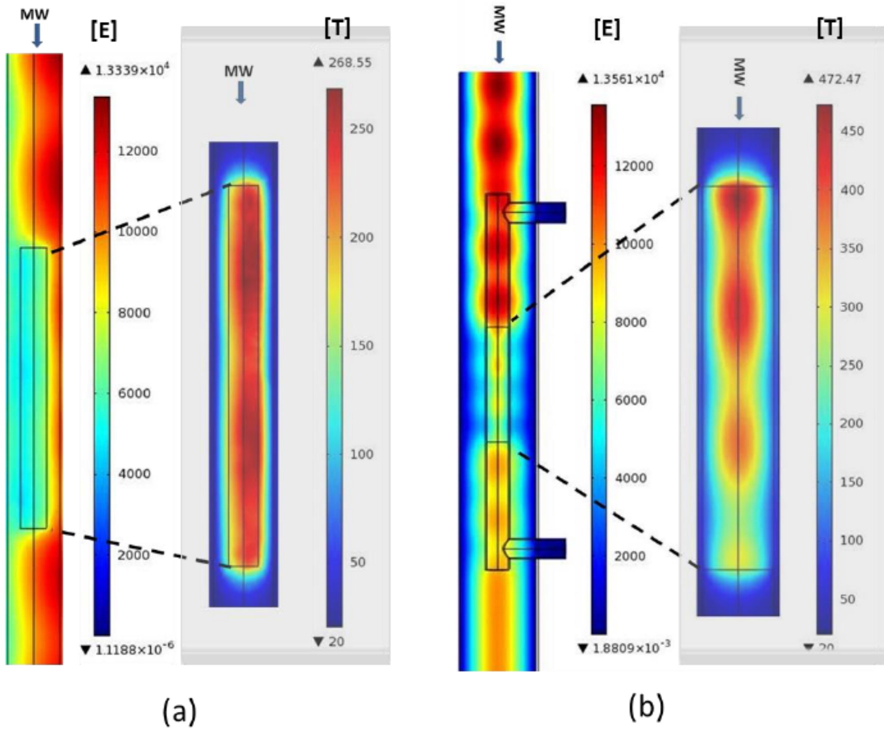

Figure 8 Electric field (*V/m*) and temperature (*℃*) in a) brick shaped catalyst bed and, b) cylindrical catalyst bed both placed in the center of the cavity (Note: different temperature scales)

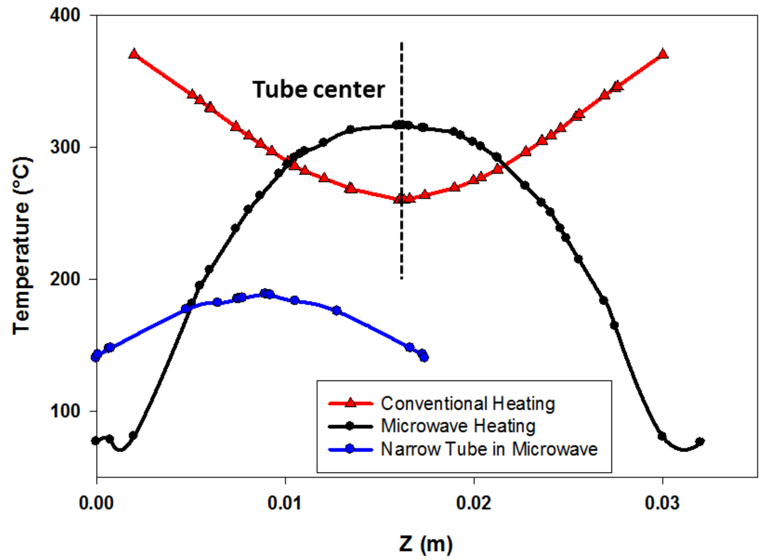

Figure 9 Temperature distribution along the centerline in z-axis (along the reactor tube radius) for microwave heating (regular sized and narrow catalyst bed) and conventional heating

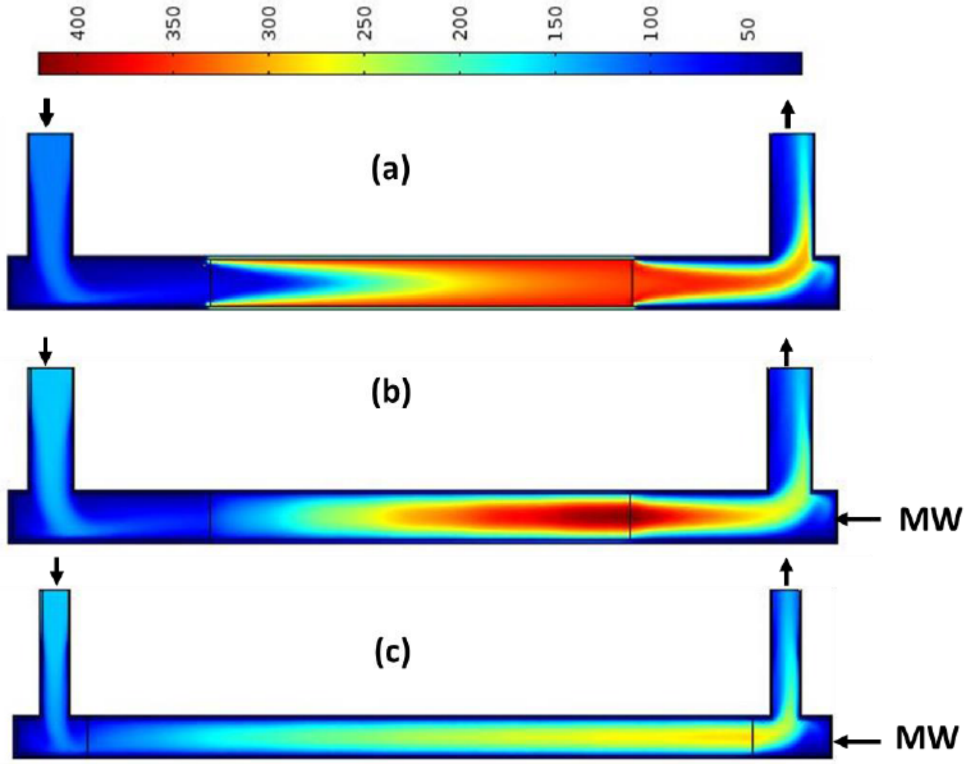

Figure 10 Longitudinal (*xz*-axis) temperature profile for (a) regular tube in conventional heating (b) regular tube in microwave (c) narrow tube in microwave

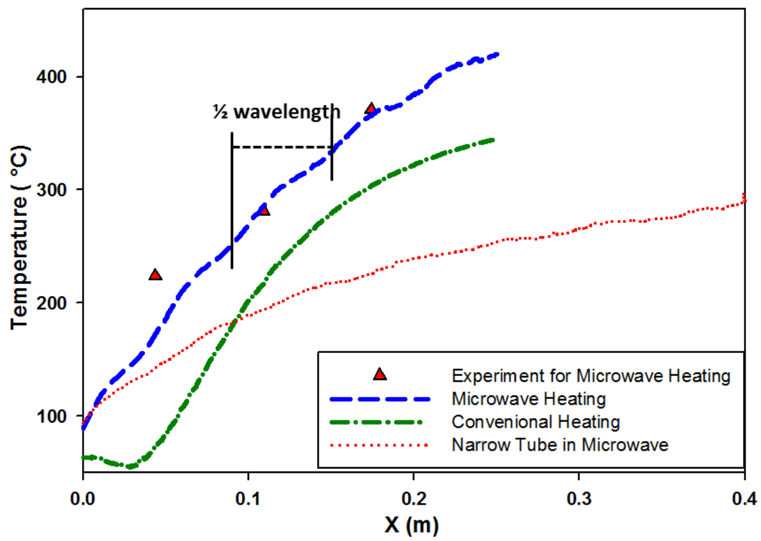

Figure 11 Temperature distribution along the centerline in *x*-axis for microwave heating (regular and narrow tube), conventional heating and experimental data (regular tube in microwave)

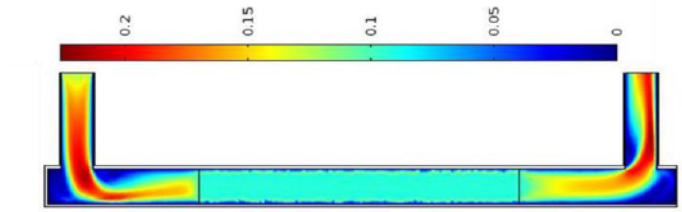

Figure 12 Velocity profile along the *zx*-axis

Numerical Modeling of Microwave Heating of A Porous Catalyst Bed

P. D. Muley[1], K. Nandakumar[2], and D. Boldor[1*]

[1]*Department of Biological and Agricultural Engineering, Louisiana State University Agricultural Center, Baton Rouge, LA 70803USA: pmuley1@lsu.edu*

[2]*Department of Chemical Engineering, Louisiana State University, Baton Rouge, LA 70803USA: nandakumar@lsu.edu*

* Correspondence: dboldor@agcenter.lsu.edu; Tel.: +1-225-578-7762149

Dorin Boldor, Ph.D. is the Charles P. Siess Jr. Professor of Engineering in the Department of Biological and Agricultural Engineering at Louisiana State University and LSU AgCenter. His expertise includes bio-energy management, electromagnetic processing methods for biofuel production and other agro-environmental applications, imaging and process control methods in bioengineering and bio-energy. He received more than $9 million in grant funds for his research projects, and published more than 75 peer-reviewed journal articles, book chapters, and proceedings.

Pranjali Muley, Ph.D. is a post-doctoral researcher with Boldor Group. She earned her PhD in December 2015 and worked as a postdoctoral research in Chemical engineering at LSU. She has over 7 years of research and development experience in biomass conversion to bioproducts using electromagnetic heating. She has a Bachelor’s degree in Chemical Engineering. Her current research projects are biomass deconstruction, developing novel catalysts for biogasoline production and computational modeling of microwave-based processes.

Krishaswamy Nandakumar, Ph.D. is a Cain Endowed Chair and Professor of Chemical Engineering at Louisiana State University. His research interests include numerical modelling of multiphase flows, computational fluid dynamics, mineral polymer and electrochemical processes including fuel cells.

ABSTRACT

A Multiphysics numerical model was developed using COMSOL Multiphysics to study the effect of size, shape and position of catalyst bed within the microwave reactor (2450 MHz). The dielectric properties of HZSM-5 catalyst were measured at different frequencies and nine different temperatures ranging from 250° - 700°K. The heat transfer in porous media was coupled with RF electromagnetics module and flow through porous media by extracting the heat source term Q for the heat transfer problem from the electromagnetics. A solid-fluid thermal non-equilibrium condition was modeled as the heat is generated within the catalyst. It was observed that sample position, shape and size of the sample, all significantly affect the heating profile and temperature gradient inside the porous media. The experimental results and the predicted temperatures were in good agreement. Microwave heating had higher total internal energy but conventional heating had lower temperature gradient after reaching steady state. Brick shaped sample heats more uniformly compared to cylindrical sample. If the radius of the sample is decreased, while maintaining the volume of the sample, microwaves penetrate deeper inside the sample, and more uniform temperature distribution is observed throughout the length of sample.

KEYWORDS: multiphysics modeling, catalytic upgrading lignin, pyrolysis, porous media

1. INTRODUCTION

Thermo-catalytic treatments of bio-oil from biomass pyrolysis (including lignin) have shown to improve biofuel quality (Muley P. D. et al. 2016). Thus, it is important to develop an efficient catalytic heating mechanism that maximizes the energy transfer. There are numerous drawbacks for conventional heating of catalyst bed reactors; amongst the most limiting one is the temperature gradient in radial heat transfer of packed bed reactors (Muley Pranjali D. et al. 2015). Since most conventional reactors are designed to provide heat at the outer region of the reactor tube, most of the energy is rapidly consumed by the outer layers of the packed bed, affecting the rate of reaction in the inner layers. This type of heat profile is especially unsuitable for upgrading of pyrolysis vapors, as the incoming vapors tend to condense on the relatively cooler catalyst area at the center of the reactor which causes catalyst fouling and a marked decrease in yield and quality of bio-oil (Muley P. D. et al. 2016). Moreover, the catalyst on the outer tubular region may heat to very high temperatures which cause the pyrolysis vapors to break down to incondensable gases (CO, CO_2, H_2, CH_4 etc.) rather than a condensable bio-oil that can be used in liquid form (Muley P. D. et al. 2016). In spite of improved heat- transfer designs, conventional heating technology lacks efficient and optimum use of imparted energy to achieve the desired uniform temperature distribution.

Microwave heating, on the other hand, induces heat at the molecular level by directly converting the electromagnetic field into heat, resulting in a temperature gradient, where the core temperature can be greater than the surface temperature (Fernández). These properties of microwave heating make it a more efficient heating method compared to conventional heating, with a conversion efficiency of electrical energy to heat that can reach 80%-85% (Lam and Chase 2012). Although there are few mechanisms that could explain the dielectric response to electromagnetic field, dipolar polarization and ionic conduction dominate at the microwave frequencies. Both these responses depend on the dielectric properties of the material (i.e. dielectric permittivity) and hold especially true for liquids, semi-solids and gases. For dry or partially dry solids without dipoles such as zeolites and carbon-based materials (commonly used as porous catalysts), the theory of dipolar rotation and ionic conduction does not entirely explain the microwave heating mechanism.

It has been proposed that in certain materials such as carbon, some charged particles (electrons) are free to move but only in a delimited region of the material. In this region, a current is induced which produces similar effect as that of ionic conduction in liquids, gases and other ionic mixtures. In the constricted region of the material, the charged particles vibrate, dissipating electromagnetic energy as heat via what is known as the Maxwell-Wagner effect (Menéndez et al. 2010). In other materials such as zeolites, the microwave heating mechanism is not extensively studied. Among the existing studies, an important one was conducted on microwave heating of zeolites which explains the heating mechanism as an ionic rattling effect within the zeolite structure (Komarneni and Roy 1986). According to another study conducted by Ohgushi et al., when hydrated zeolites were irradiated by microwaves, they initially heat due to the moisture present. Once the adsorbed moisture is completely desorbed, the dry zeolite continues to heats directly due to their lossy dielectric nature up to 500 *°C,* at which point thermal runaway occurs (Ohgushi et al. 2001).

The relation between permittivity ε (which dictates the behavior of an electromagnetic field) and dielectric constant ε' and dielectric loss factor ε'' is given by the complex equation (Gabriel et al. 1998):

$$\varepsilon = \varepsilon' - j\varepsilon'' \qquad [1]$$

Where real part (or dielectric constant) ε' is defined as the ability of the material to store imparted microwave energy and the imaginary part (or the dielectric loss factor) ε'' stands for the ability of material to convert the electromagnetic energy into heat.

Operational parameters such as microwave frequency and system's geometry, and material properties such as viscosity, density, temperature, molecular weight, concentration etc. also affect the response of material to microwave field especially those that are temperature dependent. Dielectric properties play an important role in calculating energy efficiency of the reaction process. The amount of energy absorbed and dissipated as heat can be given as (Nelson 1992):

$$P_{abs} = \sigma E^2 = 2\pi f \varepsilon_0 \varepsilon'' E^2 \qquad [2]$$

Where, P_{abs} is volumetric power absorbed (W/m^3), σ is the conductivity (S/m), f is frequency (Hz), ε_0 is the dielectric constant of the vacuum, ε'' is relative dielectric loss, E is electric field intensity (V/m).

Apart from increased heating efficiency, microwave heating of catalyst may improve catalyst performance compared to conventional heating. There are several reports in literature documenting the increased rate of reaction with the use of microwave heating (Terigar et al. 2010),(Inoue et al. 2002), (Lidstrom et al. 2001).

Due to the aforementioned potential advantages of microwave technology applied to chemistry, the technology is now extensively studied to investigate the effect of microwave heating of catalysts in endothermic reactions. Perry et al., [13] studied the effect of microwave heating of catalyst in methanol steam reforming reaction using both experimental and numerical methods (Perry et al. 2002). They developed a 1D heat transfer numerical model in a single pellet and a 2-D model for heat transfer in packed bed tubular reactor, and the experimental results validated the proposed model. Both 1D pellet model and the 2-D tubular reactor model showed elimination of radial heat transfer effects, space gradient and hot spot formation, confirming that improved performance of the catalyst in experiments was related to its more uniform heating. Other microwave heating studies report improvement in catalyst performance for heterogeneously catalyzed reactions such as conversion of methane (Ioffe et al. 1995), catalytic oxygenation of benzene (Zhang et al. 2012) attributed to better catalytic activity and improved oxidation efficiency due to dipolar polarization effects and stable bed temperatures.

In order to design an experimental set up for microwave heating of catalyst for pyrolysis vapor upgrading, it is important to understand how the catalyst can be heated in the given microwave cavity. Operational parameters such as penetration depth of the material, frequency of microwave, geometry of reactor and material properties are important parameters to be considered for the design of microwave reactors (Cablewski et al. 1994). A numerical analysis can be employed to understand the effects of these parameters on the process and provide guidance for further experimental studies. Numerous numerical studies have been conducted to study microwave heating of porous media, with most of them representing food industry applications. Rakesh et al., conducted a study to understand the temporal and spatial temperature and moisture patterns in food cooked in a combination of microwaves and hot air (Datta 2008). Nicolas et al., studied the heat and mass transfer in bread baking using COMSOL multiphysics (V. Nicolas et al. 2010). For the non-food industry related applications, Chen et al., numerically studied the effect of microwave power on catalyst bed heating and methane decomposition reaction (Chen et al. 2013).

The objective of this study was to numerically investigate the microwave and conventional heating of a porous catalyst bed in order to understand the heat and flow profiles within the reactor. The effect of size, shape and position of catalyst bed inside the microwave on the temperature attained and the overall heating profile was investigated. To our knowledge, this is the first study reporting an in depth sensitivity analysis of the effect of microwave heating in a continuous flow system for catalytic upgrading of pyrolysis bio-oil that accounts for the multiple interactions between Maxwell's equations governing EM heating, heat transfer, and flow through porous media while considering temperature dependent dielectric properties and variable configurations.

2. MODEL DEVELOPMENT

COMSOL 5.1 multiphysics software [COMSOL Inc. Boston, MA, USA] was used to solve the numerical problem with temperature dependent properties. The heat transfer and flow through porous media was coupled with RF electromagnetics module by extracting the heat source term Q for the heat transfer problem from the electromagnetics.

2.1 *Governing Equations*

Electromagnetics

The governing equation for electromagnetic wave propagation in a medium is given by Maxwell's equations (Muley Pranjali D. and Boldor 2012)

$$\nabla \cdot \vec{D} = \rho \qquad [3]$$

$$\nabla \times \vec{E} = -\frac{\partial \vec{B}}{\partial t} \qquad [4]$$

$$\nabla \cdot \vec{B} = 0 \qquad [5]$$

$$\nabla \times \vec{H} = \vec{J} + \frac{\partial \vec{D}}{\partial t} \qquad [6]$$

$$\vec{D} = \varepsilon' \varepsilon_0 \vec{E} \qquad [7]$$

$$\vec{B} = \mu' \mu_0 \vec{H} \qquad [8]$$

$$\vec{J} = \sigma_e \vec{E} \qquad [9]$$

where, E is the electric field; B is the magnetic flux density; ρ is electric charge density; J is the electric current; σ_e is electrical conductivity; D is electric displacement; ε_0 is the permittivity of free space $(8.854x10^{-12})$ F/m; H is magnetic field intensity; ε' is the relative dielectric constant; t is time (s); μ' is relative permeability of material; μ_0 is magnetic permeability of vacuum $(4\pi\ x\ 10^{-7})$ N/A^2

To determine the electric field distribution in a TE_{10} rectangular waveguide (used as a microwave cavity), a wave equation derived from Maxwell's equations is solved (Muley Pranjali D. and Boldor 2012),

$$\nabla \times \left(\frac{1}{\mu'} \nabla \times \vec{E}\right) - \frac{\omega^2}{c}(\varepsilon' - j\varepsilon'')\vec{E} = 0 \qquad [10]$$

Total volumetric power generation due to microwave is calculated by the following equation (Muley Pranjali D. and Boldor 2012)

$$Q_{gen} = \sigma_e E^2 = 2\pi f \varepsilon_0 \varepsilon'' E_{rms}{}^2 \qquad [11]$$

Q_{gen} is power absorbed from microwave, which is used as a heat generation term in Fourier equation (W/m^3), σ_e is the conductivity (S/m), f is the frequency (Hz).

Heat transfer

The source of heat was direct heating of catalyst bed due to electromagnetic heating. Generally, heat transfer in porous media is given by the following equation (Muley Pranjali D. and Boldor 2012)

$$(\rho C_p)_{eq} \frac{\delta T}{\delta t} + \rho C_p u \cdot \nabla T = \nabla \cdot \left(k_{eq} \nabla T\right) + Q_{gen} \qquad [12]$$

Where ρ and C_p are the fluid density and heat capacity of the fluid, whereas $(\rho C_p)_{eq}$ is defined as the equivalent volumetric heat capacity at constant pressure. k_{eq} is the equivalent thermal conductivity, u is defined as the Darcy's velocity expressed as volume flow rate per unit cross sectional area; Q_{gen} is the heat source. The equivalent terms are related to the respective property of the solid and the fluid. Thus, k_{eq} is the equivalent solid-fluid conductivity given by (Multiphysics 2015),

$$k_{eq} = \theta_s k_s + \theta_L k \qquad [13]$$

And the volumetric heat capacity for solid-fluid system is given by (Multiphysics 2015),

$$(\rho C_p)_{eq} = \theta_s \rho_s C_s + \theta_L \rho C_p \qquad [14]$$

Where, $\theta_s + \theta_L = 1$

Where, θ_s and θ_L are volume fractions of solid and fluid (porosity) material respectively. These equations assume local thermal equilibrium within the solid and fluid material within the porous body. However, since the heat is generated within the porous material, this assumption is not valid and the solid and fluid temperatures in the porous domain are not in equilibrium. A local thermal non-equilibrium condition should be defined for the solid and fluid interaction within the porous structure. This is achieved by coupling the heat equations in the solid and fluid subdomains through a transfer term proportional to the temperature difference between the fluid and the solid. The Local Thermal Non-Equilibrium (*LTNE*) Equations are given as follows;

For solid phase (Multiphysics 2015);

$$\theta_s (\rho c_p)_s \frac{\delta T_s}{\delta t} = \theta_s \nabla \cdot (k_s \nabla T_s) + \theta_s q_s + h(T_f - T_s) \qquad [15]$$

For fluid phase (Multiphysics 2015);

$$\theta_L(\rho c_p)_f \frac{\delta T_f}{\delta t} + (\rho C_p)_f u \cdot \nabla T_f = \theta_L \nabla \cdot (k_f \nabla T_f) + \theta_L q_f + h(T_s - T_f) \quad [16]$$

Where, ρ is the density, C_p is the heat capacity, k_s and k_f are solid and fluid thermal conductivities, q is the interstitial convective heat transfer coefficient, u is the velocity and h is the heat transfer coefficient. The critical step in solving this equation is the determination of heat transfer coefficient, h. There are numerous studies reported which have established a correlation for appropriate value of h (Bejan 1995; Alazmi and Vafai 1999; Minkowycz et al. 1999; Saito and de Lemos 2005). In general, heat transfer coefficient is given by $h = a_{fs}h^*$, where a_{fs} is the specific surface area given by $a_{fs} = 6(1 - \varphi)/d_p$, and h^* is given as;

$$\frac{1}{h^*} = \frac{d_p}{Nu_{fs}k_f} + \frac{d_p}{\beta k_s} \quad [17]$$

Where d_p is the particle diameter, Nu_{fs} is the fluid to solid Nusselt number, β is 10 for spherical particles, Nusselt number for the solid to fluid interface is dependent on Reynolds number. For $R_e > 100$ an expression for Nusselt number is given by (Handley and Heggs 1968);

$$Nu_{fs} = \left(\frac{0.255}{\varphi}\right) P_r^{1/3} Re_p^{2/3} \quad [18]$$

This equation is valid for catalyst bed packing of various shapes including spherical, cylindrical and plate shaped packings (Handley and Heggs 1968). In our method, the COMSOL multiphysics software evaluates the Reynolds number based on the velocity in the porous region. There are various other parameters that affect the heat transfer between solid and fluid in the porous region, such as the effect of turbulent and transient flows, variable porosity, thermal dispersion as well as the effects of pressure and viscous dissipation. These additional effects were not considered in the present study. The heat transfer in open regions was solved using regular conduction convection equations as applicable.

Free and porous media flow

The flow of gases through the free and porous region of the tube was solved. The flow of gases through open regions in described by Navier-Stokes equation (Multiphysics 2015)

$$\rho_m \left(\frac{\partial_u}{\partial_t} + u \cdot \nabla u\right) = -\nabla P + \mu \nabla^2 u + F \qquad [19]$$

Continuity equation is (Multiphysics 2015)

$$\nabla \cdot \vec{u} = 0$$

Where; u is velocity of fluid in (*m/s*); μ is viscosity in ($P_a{\cdot}s$); P is pressure (*Pa*); F is other forces such as gravity or centrifugal force per unit volume (N/m^3)

Whereas, Brinkman equation is used to describe the flow of gases through porous matrix and is given by (Multiphysics 2015);

$$\frac{\rho}{\varepsilon_p}\left(\frac{du}{dt} + (u \cdot \nabla)\frac{u}{\varepsilon_p}\right) = \left[-\nabla \mathrm{P} + \frac{\mu}{\varepsilon_p}\nabla^2 u - \frac{2\mu}{3\varepsilon_p}\nabla^2 u\right] - \left(\mu k^{-1} u + \beta_F |u|^2 + \frac{Q_{br}}{\varepsilon_p^2} u\right) + F \quad [20]$$

$$\rho \nabla \cdot u = Q_{br}$$

Where, ε_p is the porosity, k is the relative permeability, β is the effective viscosity and Q_{br} is the total discharge.

2.2 ***Assumptions***

High frequency electromagnetism module was coupled with heat transfer in porous medium and flow through porous media using COMSOL Multiphysics 5.1. To reduce the complexity of the model, certain assumptions were made for the model development.

- The porous media was considered uniformly porous throughout the catalyst bed.
- Thermal properties were constant with changing temperature
- No chemical reaction or phase change occurred.

- Quartz tube with the catalyst bed placed inside the microwave was completely transparent to the microwaves.
- Waveguide walls are perfect conductors with no absorption of microwave energy by the cavity or air.
- Average inlet velocity was *0.125 m/s* as measured during experimental validation runs

2.3 *Geometry*

A *3-D* geometry of a pilot scale microwave waveguide was built in COMSOL 5.1 (**Figure 1**). The setup consisted of a 1.2 kW, 2450 MHz power source, connected to an aluminum waveguide of dimensions *1.37 m* long, *0.106 m* wide and *0.053 m* deep (Industrial Microwave Systems (IMS), Inc. Morrisville, NC), shorted at the far end. The porous catalyst bed was placed inside a quartz tube with *0.014 m* internal radius and *0.49 m* length sitting at the center of the waveguide. The catalyst bed has a *0.014 m* radius and is *0.15 m* long initially placed at the center of the quartz tube.

2.4 *Boundary conditions*

Electromagnetic Waves

The microwave power was set at *400 W* for all combinations investigated. The electromagnetics wave module was active in all domains. The microwave energy was supplied to the cavity through the rectangular waveguide at port one in TE_{10} mode electric. The dielectric properties of the catalyst bed were measured as described in section 3.1 and defined in the model, the dielectric properties were temperature dependent and given by equation $0.065*exp(-0.002*T)$(where T is temperature in °C). Scattering boundary conditions were defined at the outlet and inlet of the quartz tube in order to avoid undesired reflections and perturbations in the field caused by sudden discontinuity in the waveguide. A continuity boundary condition was applied to all the internal boundaries of the domains.

Heat Transfer in Porous Media

Heat transfer in porous media module was coupled with the electromagnetics and flow module. The porous matrix was the catalyst bed whose porosity was measured in lab to be 0.67. The density (*720 kg/m³)*, thermal conductivity (*0.12 W/m²K)* and specific heat (*1369 J/kg °K)* of the material were obtained for material properties from Zeolyst International. The heat source Q_{gen} was set as the electromagnetic power loss density calculated from electromagnetics module. Convective cooling was defined for the outer walls of the waveguide and quartz tube walls. Conjugate heat transfer was active in all domains.

Free and Porous Media Flow

The laminar flow module was active in the quartz tube only. The inlet velocity of the fluid was measured as *0.125 m/s,* and the inlet temperature was *150 °C*. The porosity was determined to be *0.67* and was assumed to be uniform throughout the catalyst bed.

2.5 *Mesh Generation*

The element size requirement for solving the electromagnetic problem is that the maximum grid element size (S_{max}) should be less than half the wavelength. This requirement is known as the Nyquist criterion and is defined as,

$$S_{max} < \frac{\lambda}{2} = \frac{c}{2f\sqrt{\varepsilon'\mu'}} \qquad [23]$$

Where, λ is the wavelength (*m*), f is the frequency (*Hz*), c is the speed of light in vacuum (*m/s*), ε' is the relative dielectric constant, and μ' is the relative permeability. Based on this criterion, the default fine mesh size was used where the maximum element size was set conservatively at 0.00614 *m* in the waveguide and the maximum element size was set to *0.00116 m* for quartz tube and porous media. The models were tested at 3 different mesh sizes of (cavity element number, reaction tube element number) = (243599, 32229), (306159, 41004), (490640, 81895) and the grid independence for both microwave and conventional heating models was established (**Figure 2**)

The distribution of temperature along the centerline of the catalyst bed in *x* direction is plotted in **Figure 2**. The difference in temperature distribution between all three grid sizes is low, but it is especially negligible between the second (306159, 41003) and third grid size (490640, 81895) and satisfies the grid independence. Thus, further studies were conducted at (490640, 81895) grid size.

2.6 *Solver used*

The frequency domain was used to solve the wave equation in the radio frequency module. The frequency was set to *2.45 GHz*, which is the operating frequency of the microwave. The stationary solver was used to solve heat transfer and fluid flow equations in porous media to obtain the temperature profiles.

2.7 *Methods*

An initial study was conducted to study the effect of sample size, shape and position inside the microwave cavity. A numerical model was developed using COMSOL Multiphysics 5.1 studying the effect of electromagnetic irradiation on porous catalyst bed for this purpose. Gas flow through the porous media was not considered for the preliminary study. The catalyst used is a dielectric material and readily heats up in a microwave reactor. Since the position of catalyst bed inside the reactor plays a crucial role in the uniform heating of catalyst, a sensitivity analysis was performed using five different positions (**Figure 3**);

- center of the waveguide $(z = 0)$
- base of the waveguide ($z=-0.03m$)
- upper edge of the waveguide $z=0.03m$
- $z=-0.01\ m$
- $z=-0.02m$.

The effect of size of the catalyst bed was also tested by designing a smaller diameter tube while maintaining the volume of the catalyst bed. The new design also underwent a sensitivity analysis for 3 different positions; a) center of the waveguide $z=0$, b) $z=-0.01$ and, c) $z=-0.02$. Two shapes of catalyst bed (a) rectangular block and, (b) cylindrical were investigated to study the effect of shape on the temperature profile.

A more thorough secondary study with experimental validation, was performed where the flow of gas through the quartz tube was taken into account. The conjugate heat transfer equation was solved for porous domain where the solid and fluid temperatures are not in equilibrium. The average velocity of the incoming gas was *0.125 m/s* to correspond with the existing experimental conditions as measured. As measured during experimental runs, the incoming gas temperature was *150 °C* and external atmospheric temperature was *25 °C*. A conventional heating model was also developed for comparison. Experimental temperatures at three locations were also measured for model validation. Due to limitations with temperature measurements within the microwave cavity, only three locations were chosen for temperature measurement using IR pyrosensors and thermal camera. The IR sensors were calibrated for quartz glass transparency and emissivity.

3. RESULTS AND DISCUSSION

3.1 *Dielectric properties of HZSM-5 catalyst at different temperatures*

The dielectric properties play an important role in the microwave heating of material. Knowledge of dielectric properties of material under treatment gives a clear understanding of how a particular material will heat under the influence of electromagnetic waves. Depending on the material, dielectric properties may be temperature and frequency dependent.

The dielectric properties of HZSM-5 powder was measured using an Agilent ENA series E5071C Network Analyzer and Agilent 85070E dielectric probe kit (Agilent Technologies, Inc. Santa Carla, CA) using a slim form open-ended probe method in a 201-point frequency sweep from *280 MHz* to *4500 MHz*. The network analyzer was controlled by Agilent 85070E dielectric kit software (Agilent Technologies, Inc. Santa Carla, CA) and calibrated using the 3-point method (short-circuit, air and water at *25 °C*). The NaZSM-5 catalyst was calcined in air at *550 °C* for *5.0 h* to convert NaZSM-5 to HZSM-5. The powder was then filled in a tube surrounded with a heating tape. Dielectric properties were measured at nine different temperatures ranging from *298 ° - 643 °K*.

Figure 3a,b show change in dielectric constant and dielectric loss at different frequencies and different temperatures. While no significant difference was observed with the change in frequency, the dielectric properties were temperature dependent. **Figure 4c,d,e** shows the electrical conductivity, dielectric loss and dielectric constant values at *2450 MHz* frequency for different temperatures. Electric conductivity is given by

$$\sigma = 2\pi f \varepsilon_0 \varepsilon'' \qquad [24]$$

Where, f is frequency (*Hz*), ε_0 is the dielectric constant of the vacuum, ε'' is relative dielectric loss of material.

For a material to undergo dielectric heating under microwave radiation, the conductivity of the material should be higher that 0; i.e. the electric field flows through the material. When electric field flows through the material, some of the energy is converted to heat. Materials with $\sigma = 0$ are called lossless material (air, vacuum) and those with very high conductivities ($\sigma >> 0$), are called conductors such as metals. Materials with medium range conductivities ($\sigma > 0$) are called lossy materials and they readily heat in a microwave. Since the conductivity of catalyst is slightly greater than 0, it is categorized as a lossy material (F**igure 4**).

3.2 *Primary Study*

3.2.1 *Effect of position of catalyst bed*

In general, due to the specific propagation of EM waves in the microwave cavities partially filled with a lossy or conductive materials, it is expected that the distribution of the EM field both in the void spaces (air, vacuum) and in the lossy material (load) will be dependent on the specific location and geometry of the load in the cavity. Hence the effect of position of sample on heat profile inside the microwave cavity was investigated. We studied three different locations of dielectric material a.) center of the cavity ($z=0$), b.) base of the waveguide $z=-0.03$ m and, c.) top of the waveguide $z = 0.03\ m$. (**Figure 5**)

In case where the dielectric catalyst bed is placed at the center of the cavity (**Figure 5a**), the electric field intensity is observed to decrease as the microwaves travel through the dielectric material. The electric field intensity is lower inside the dielectric material than in the void. The temperature profile is consistent with that of the electric field since microwave heating rate of a dielectric material is proportional to the square of the electric field. Maximum electric field intensity in the catalyst bed was *13561 V/m* and the corresponding temperature was *472 ºC* (**Figure 5a**). It is also observed that most of the energy is absorbed at front end of the catalyst bed located towards the incident wave as expected. Due to the skin-depth effect, as the thickness of the sample increases, current density decreases, resulting in temperature decay along the wave propagation direction (Ratanadecho et al. 2002).

When the catalyst bed is moved close to the base of the waveguide by *3 cm*, most of the electric field is concentrated only in the upper region of the catalyst bed, leaving the base of the catalyst bed unheated (**Figure 5b**). Maximum electric field intensity in the catalyst bed was *14000 V/m* in the waveguide and 10000 *V/m* in the catalyst bed, similar to the case when the catalyst bed is placed in the center of the cavity, and the highest corresponding temperature is *654.46 ºC*. For the same incident power, higher temperature is achieved when the bed is close to the base of the waveguide compared to the center because only a fraction of the catalyst is absorbing the energy. Since some of the catalyst material is outside the electric field area, the energy absorbed is limited to the upper part of the catalyst bed (Vadivambal and Jayas 2010). Similar electric field distribution and temperature profile is observed when the catalyst bed is positioned close to the top of the waveguide (*z=0.03m*) (**Figure 5c**). Since most of the energy is concentrated in the lower part of the catalyst bed, the upper catalyst area is not heated. The maximum electric field intensity in the catalyst bed was *9000 V/m* and the corresponding maximum temperature achieved is *684.47 ºC*. These results were in agreement with the literature where Funawatashi and Suzuki (2003) studied the effect of sample position on the electric and temperature fields (Funawatashi and Suzuki 2003). They observed that electric field greatly depends on the position of a dielectric material and consequently affect the heating rate. Rattanadecho et al., (2009) concluded that the rate of heating of dielectric material significantly changes with position of the material in the microwave waveguide (Cha-um et al. 2009). For all three catalyst position, non-uniform temperature profile was observed. Uneven heating in the microwave cavity is a result of two phenomenon; due to standing wave pattern and due to rapid decay of microwaves and uneven exposure of the catalyst mass to the incident microwaves (Cha-um et al. 2009; Vadivambal and Jayas 2010).

Figure 6 shows the temperature profile in YZ direction at the center of the catalyst bed for five different catalyst bed positions. High temperature zone is at the center when the catalyst bed is positioned at the center of the waveguide (**Figure 6b**). However, as the position of the catalyst bed is changed, the hot spot location changes. Moreover, 320 °C temperature was achieved for the center position as opposed to 500 °C when the catalyst bed was either at the top (**Figure 6a**) or bottom (**Figure 6e**) of the waveguide. This could be attributed to the fact that for the bed position closer to the waveguide wall, a significant part of the catalyst bed remains unheated, creating an undesirably large temperature gradient inside the bed.

We also studied the effect on temperature profile when the catalyst bed is moved slightly off center (10 mm and 20 mm off center) (**Figure 6**). For position z= *10 mm* off center, the highest temperature noted was 600 °C (**figure 6c**). This temperature dropped significantly to only 260 °C when the catalyst was moved *20 mm* off center (to a range of 100 – 260 °C). We also observed that the temperature gradient greatly reduces when the catalyst bed position is *20 mm* off from the center (**Figure 6d**). These observations could be attributed to the smaller sample size which causes arbitrary wave reflection resulting in multimode of field pattern (Cha-um et al. 2009). For a closed microwave cavity like the one studied here, the occurrence of standing waves creates uneven heating. Some methods to cancel or minimize the effect of standing waves pattern is to move the sample continuously, change the size of cavity or change the size and/or position of sample within the cavity. Placing the sample 20 mm off center might have minimized this effect, resulting in lower temperature gradient.

3.2.2 *Effect of catalyst bed dimensions*

We studied the effect of sample configuration on microwave heating. The catalyst bed diameter was reduced while keeping its volume constant via increased bed length. The new sample was positioned at three different locations (center – z = 0, 10mm off center $z=-0.01$ and 20 mm off center $z=-0.02$) inside the waveguide to test the effect of position. These positions were selected based on the previous results obtained for larger diameter tube (section 3.2.1). Higher temperature was observed at the front end where the microwaves enter the catalyst bed, but this temperature was lower (by as much as half when located at the center of the waveguide) than that observed in the thicker catalyst bed (**Figure 7**).

As opposed to the earlier model with larger diameter catalyst bed, fewer cold regions were observed for the new geometry (**Figure 7**). This can be explained by the fact that since the thickness of the sample decreased and length increased, the microwave absorption was much softer and more evenly distributed along the length of the bed, as opposed to being absorbed all upfront in the thicker catalyst bed. The ratio of penetration depth to the bed diameter changed and microwaves were absorbed along the complete length of the catalyst bed. Thus, non-uniform heating due to rapid decay of microwaves in the incident direction can be controlled by changing the dimensions of the dielectric sample in this particular configuration. A general trend is that as the sample volume increases, the rate of temperature rise decreases. However, if the thickness of the sample is smaller than the penetration depth of the sample, even with larger volume, a higher rate of temperature rise can be obtained (**Figure 9**).

If the penetration depth of the sample is greater than the thickness of the sample, it causes interference to the waves that are reflected from sample-air interface due to the difference in air and sample dielectric properties. This reflection and transmission at the interfaces contribute to a resonance of standing waves inside the porous sample and the electric field distribution does not decays exponentially from the surface, as expected (Muley Pranjali D. and Boldor 2012), eventually decreasing the rate of temperature rise (Cha-um et al. 2009). It is also noted that the temperature distribution was more uniform when the sample was placed 20 mm away from the center (**figure 7**).

3.2.3 *Effect of sample shape*

We studied the effect of having a rectangular brick shaped sample and compared the results with the cylindrical sample of same volume. More uniform heating was observed for bricked shaped sample compared to cylindrical sample. A sharp rise in temperature was observed in the z direction at the center of the sample (**figure 8**). Cylindrical sample showed higher temperature at the center and cooler temperatures zones at the margins, as well as much more variability in the wave incident direction (x-axis). For cylindrical samples, less of the incident microwave energy is absorbed at the surface prior to reaching the center. Hence a higher concentration of microwave energy is focused at the center causing more heating at the core. This is especially true for narrow diameter tubes where the distance travelled through the lossy portion is smaller. These results were in agreement with literature results comparing three different shapes; cylindrical, brick and hexagonal prism. Vilayannur et al., concluded that for a cylindrical shaped sample, the heating is mostly concentrated at the center of the samples as opposed to the corners in case of brick-shaped samples (Vilayannur et al. 1998). While we did not observe higher heating at the corners for brick shaped sample, the temperature distribution was much more uniform with heating taking place at the corners as well as the center of the sample.

3.3 *Experimental validation and comparison to conventional heating*

3.3.1 *Temperature profile*

A thorough secondary study includes the effect of gases flowing through the porous catalyst bed. **Figure 10** shows the temperature profiles for microwave and conventionally heated catalyst bed. The temperature of the fluid entering the quartz tube was *150 °C*. For the conventional heating model, the walls of catalyst bed were maintained at a constant temperature of *370 °C*. The temperature along the x-axis is plotted (**Figure 11**). The temperature at the core of the catalyst bed is higher for microwave heating and lower towards the wall. However, as expected for conventional heating, higher temperature is obtained at the walls of the catalyst bed and the temperature reduces towards the center. Due to the local thermal non-equilibrium condition, the heat is carried by the fluid and the exit temperature of the fluid is higher than the inlet temperature. The highest temperature achieved by microwave heating was *420 °C* towards the side of the catalyst bed exposed to the incident microwaves.

Numerically predicted temperature was compared to the experimental data obtained during microwave bio-oil vapor upgrading runs using pine sawdust as biomass as previously described (Muley P. D. et al. 2016). Temperature was measured at three different locations in the *X*-direction along the quartz tube. An IR thermocouple and a thermal camera were used for temperature measurement. The numerical predictions were a good match (within 5%) with the experimental temperature results (**Figure 11**). Any discrepancies between the numerical model and the measured temperature of the catalyst bed could be mainly due to the assumption of average flow rate in the model. Since, in reality, the flow rate varies over the time as gas is generated within the system during reactions. Moreover, other external factors such as, local super-heating in the microwave, effect of coke deposition and poisoning of catalyst bed was not precisely modeled and could have affected the accuracy of the model.

A steady rise of temperature (as averaged in the *YZ* plane) is observed for both microwave and conventional heating in *X*-direction (**figure 11**). The temperature profile in z-direction shows a wall to wall temperature gradient within the catalyst bed for both microwave and conventional heating (**figure 9**). The temperature gradient is observed to be from the walls towards the center of the catalyst bed for conventional heating, as expected. The microwave temperature gradient is inversed, as also noted and discussed in the section 3.2 on the model without the gas flow. An effect of reaction kinetics should also be modeled for predicting the temperature profiles within the microwave system accurately. The changes in thermal conductivity and other thermodynamic parameters due to formation of new products and intermediates should be accurately modeled for precision.

3.3.2 *Velocity profile*

The flow was modeled across the porous catalyst bed. The gas inlet velocity was *0.125 m/s*. The velocity profile in longitudinal direction (*xz*- direction) was plotted. The velocity profile was consistent with the boundary conditions. The porous bed was defined as uniformly porous and a drop in velocity was observed in this region. A small recirculation region was also observed at the back ends of the geometry where the vertical tubes meet the horizontal tube. The highest velocity obtained was *0.22 m/s* (**figure 12**).

3.3.3 *Effect of tube diameter*

Similar to the no flow conditions, when the diameter of the tube was reduced to *0.02 m* for narrow tube from *0.028 m* for regular tube and the length was increased from *0.25 m* to *0.4 m*, more uniform temperature distribution was observed (**figure 10**). The overall temperature range as lower for the narrow tube (*20 °C* to *284 °C*) compared to that for the bigger diameter shorter tube (*20 °C* to *420 °C*). A temperature plot across *x* axis was plotted for both tubes (**figure 11**). The temperature in the narrow tube increases to *284 °C* in about *0.1 m* of the tube length and remains steady at that temperature for the remainder of the length, whereas a steady increase is observed for the shorter tube.

4. CONCLUSION

A Multiphysics numerical model studying the microwave heating of porous catalyst bed was developed using COMSOL Multiphysics 5.1. The effect of sample shape, size and position on microwave heating of porous catalyst bed was studied. The model was validated against the experimental data. The temperature profiles obtained from microwave heating was compared to that obtained from conventional heating profile. It was observed that sample position, shape and size of the sample, all significantly affect the heating profile and temperature gradient inside the porous media. Samples placed 20mm away from the center heat more uniformly compared to samples placed at the center, higher temperatures are achieved when the sample is placed 10mm away from the center. This is because stronger resonance effects occur due to disorderly wave reflections within the samples. The experimental results and the predicted temperatures were a close match. Microwave heating had higher total internal energy but conventional heating had lower temperature gradient after reaching steady state. This type of numerical modeling can be used to optimize the process parameters and design an efficient process depending on the ease of operation and manufacturing and the cost efficiency.

ACKNOWLEDGEMENT

The authors would like to acknowledge LSU's Department of Chemical Engineering, LSU's Department of Biological and Agricultural Engineering, LSU's Center for Computation and Technology, LSU Agricultural Center, and USDA NIFA Hatch Program [project number

LAB #94146], for their support of this project. Financial support was provided by US NSF CBET (award #1437810), US NSF OIA (award #1632854), and Louisiana Board of Regents (#Louisiana Board of Regents Support Fund (award #LEQSF(2015-17)-ENH-TR-01). Published with the approval of the Director of the Louisiana Agricultural Experiment Station as manuscript #2018-232-31870.

REFERENCES

Alazmi B, Vafai K. 1999. Analysis of Variants Within the Porous Media Transport Models. J Heat Transfer. 122(2):303-326.

Bejan A. 1995. Convection heat transfer. John Wiley & Sons, Incorporated.

Cablewski T, Faux AF, Strauss CR. 1994. Development and application of a continuous microwave reactor for organic synthesis. The J. org. chem. 59(12):3408-3412.

Cha-um W, Rattanadecho P, Pakdee W. 2009. Experimental analysis of microwave heating of dielectric materials using a rectangular wave guide (MODE: TE10) (Case study: Water layer and saturated porous medium). Exp Therm Fluid Sci. 33(3):472-481.

Chen W-H, Liou H-J, Hung C-I. 2013. A numerical approach of interaction of methane thermocatalytic decomposition and microwave irradiation. Int J Hydrogen Energ. 38(30):13260-13271.

Datta VRaAK. 2008. Coupled Electromagnetics- Multiphase Porous Media Model for Microwave Combination Heating. Excerpt from the Proceedings of the COMSOL Conference Boston 2008

Fernández, Yolanda; Arenillas, Ana; Menéndez, J. Ángel. Microwave heating applied to pyrolysis [Book Chapter]. Advances in Induction and Microwave Heating of Mineral and Organic Materials. 31:30.

Funawatashi Y, Suzuki T. 2003. Numerical analysis of microwave heating of a dielectric. Heat Transfer—Asian Research. 32(3):227-236.

Gabriel C, Gabriel S, Grant EH, Halstead BSJ, Mingos DMP. 1998. Dielectric parameters relevant to microwave dielectric heating. Chem Soc Rev. 27(3):213-223.

Handley D, Heggs PJ. 1968. Momentum and Heat Transfer Mechanism in Regular Shaped Packings [Article]. Trans. of the Institution of Chemical Engineers and the Chemical Engineer. 46(9):T251-&. English.

Inoue C, Hagura Y, Ishikawa M, Suzuki K. 2002. The dielectric property of soybean oil in deep-fat frying and the effect of frequency. J Food Sci. 67(3):1126-1129.

Ioffe MS, Pollington SD, Wan JKS. 1995. High-Power Pulsed Radio-frequency and Microwave Catalytic Processes: Selective Production of Acetylene from the Reaction of Methane over Carbon. J Catal. 151(2):349-355.

Komarneni S, Roy R. 1986. Anomalous microwave melting of zeolites. Mater Lett. 4(2):107-110.

Lam SS, Chase HA. 2012. A Review on Waste to Energy Processes Using Microwave Pyrolysis [Article]. Energies (19961073). 5(10):4209-4232.

Lidstrom P, Tierney J, Wathey B, Westman J. 2001. Microwave assisted organic synthesis - a review. Tetrahedron. 57(45):9225-9283.
Menéndez JA, Arenillas A, Fidalgo B, Fernández Y, Zubizarreta L, Calvo EG, Bermúdez JM. 2010. Microwave heating processes involving carbon materials. Fuel Process Technol. 91(1):1-8.
Minkowycz WJ, Haji-Sheikh A, Vafai K. 1999. On departure from local thermal equilibrium in porous media due to a rapidly changing heat source: the Sparrow number. Int J Heat Mass Transfer. 42(18):3373-3385.
Muley PD, Boldor D. 2012. Multiphysics Numerical Modeling of the Continuous Flow Microwave-Assisted Transesterification Process. J Microw Power Electromagn Energy. 46(3):139-162.
Muley PD, Henkel C, Abdollahi KK, Boldor D. 2015. Pyrolysis and Catalytic Upgrading of Pinewood Sawdust Using Induction Heating Reactor. Energy Fuels.
Muley PD, Henkel CE, Aguilar G, Klasson KT, Boldor D. 2016. Ex situ thermo-catalytic upgrading of biomass pyrolysis vapors using a traveling wave microwave reactor. Appl Energ. 183:995-1004.
Multiphysics C. 2015. Reference Manual, Version 5.0. Google Scholar.
Nelson SO. 1992. Correlating Dielectric Properties of Solids and Particulate Samples Through Mixture Relationships Trans ASAE. 35(2):625-629.
Ohgushi T, Komarneni S, Bhalla A. 2001. Mechanism of Microwave Heating of Zeolite A. J Porous Mater. 8(1):23-35. English.
Perry WL, Datye AK, Prinja AK, Brown LF, Katz JD. 2002. Microwave heating of endothermic catalytic reactions: Reforming of methanol. AlChE J. 48(4):820-831.
Ratanadecho P, Aoki K, Akahori M. 2002. A numerical and experimental investigation of the modeling of microwave heating for liquid layers using a rectangular wave guide (effects of natural convection and dielectric properties). Appl Math Model. 26(3):449-472.
Saito MB, de Lemos MJS. 2005. A Correlation for Interfacial Heat Transfer Coefficient for Turbulent Flow Over an Array of Square Rods. J Heat Transfer. 128(5):444-452.
Terigar BG, Balasubramanian S, Lima M, Boldor D. 2010. Transesterification of soybean and rice bran oil with ethanol in a continuous-flow microwave-assisted system: yields, quality, and reaction kinetics. Energy Fuels. 24:6609-6615.
V. Nicolas PS, PG, VJ, LB, JPP. 2010. Modeling Heat and Mass Transfer in Bread during Baking. Excerpt from the Proceedings of the COMSOL Conference 2010 Paris.
Vadivambal R, Jayas DS. 2010. Non-uniform Temperature Distribution During Microwave Heating of Food Materials—A Review. Food Bioprocess Technol. 3(2):161-171. English.
Vilayannur RS, Puri VM, Anantheswaran RC. 1998. Size and Shape Effect on Non-Uniformity of Temperature and Moisture Distributions in Microwave Heated Food Materials: Part I Simulation. J Food Process Eng. 21(3):209-233.
Zhang YC, Bo LL, Wang XH, Liu HN, Zhang H. 2012. Study on catalytic oxidation of benzene by microwave heating. Huan jing ke xue 33(8):2759-2765. chi.

List of Figures

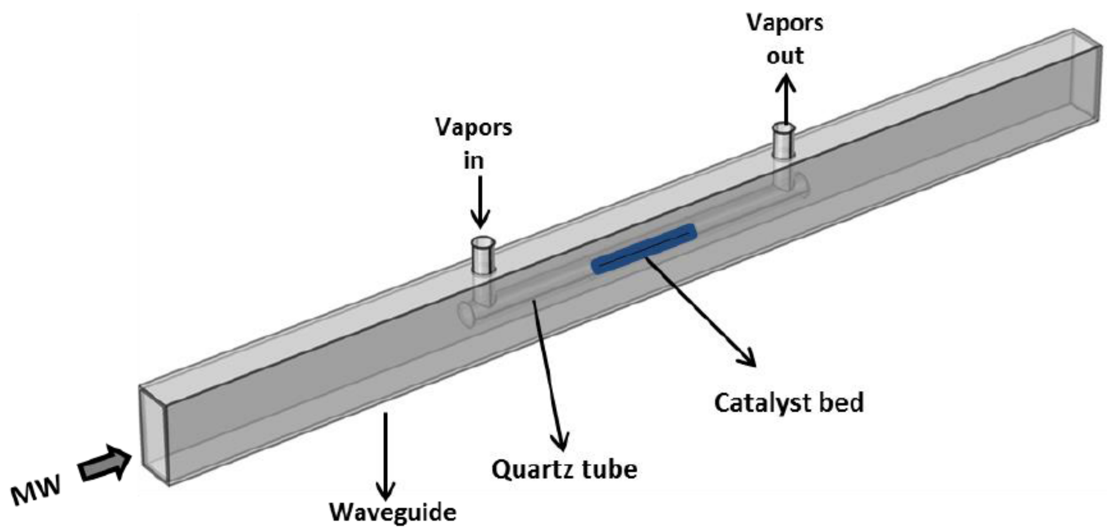

Figure 1 Geometry of microwave system used to heat porous catalyst bed

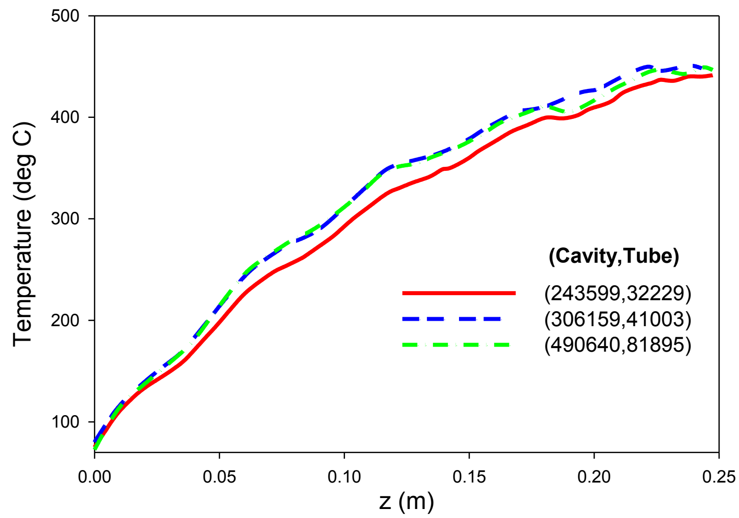

Figure 2 Temperature distributions along the centerline of the reaction tube at three different grid systems

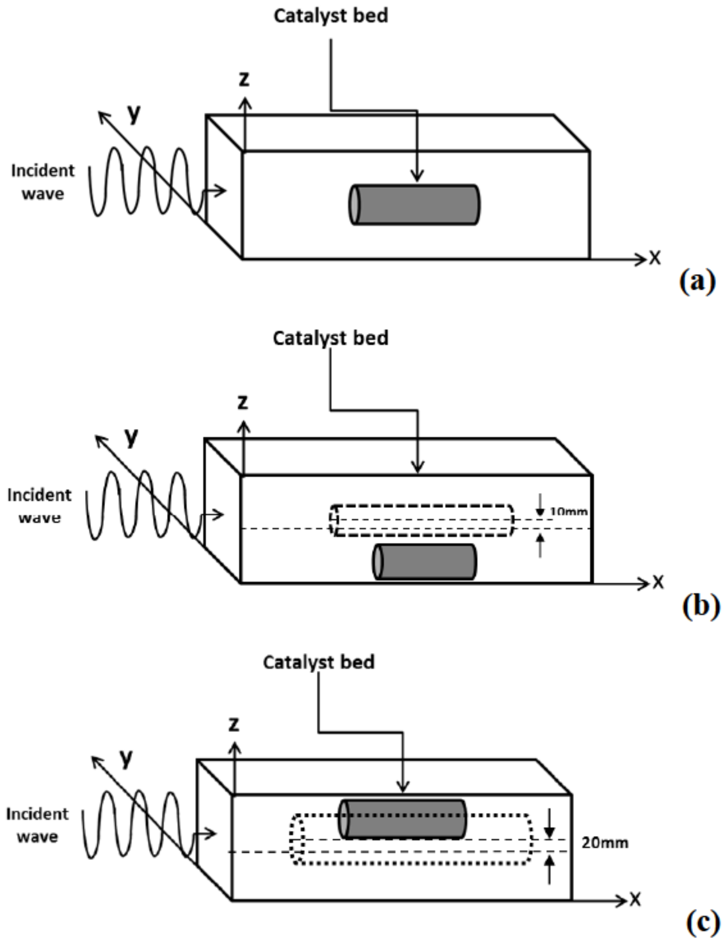

Figure 3 Position of catalyst bed within the waveguide a) center ($z=0$), b) base ($z = -0.03$) (dotted line showing narrow tube *10 mm* away from center), c) top ($z = 0.03$) (dotted line showing narrow tube *20 mm* away from center)

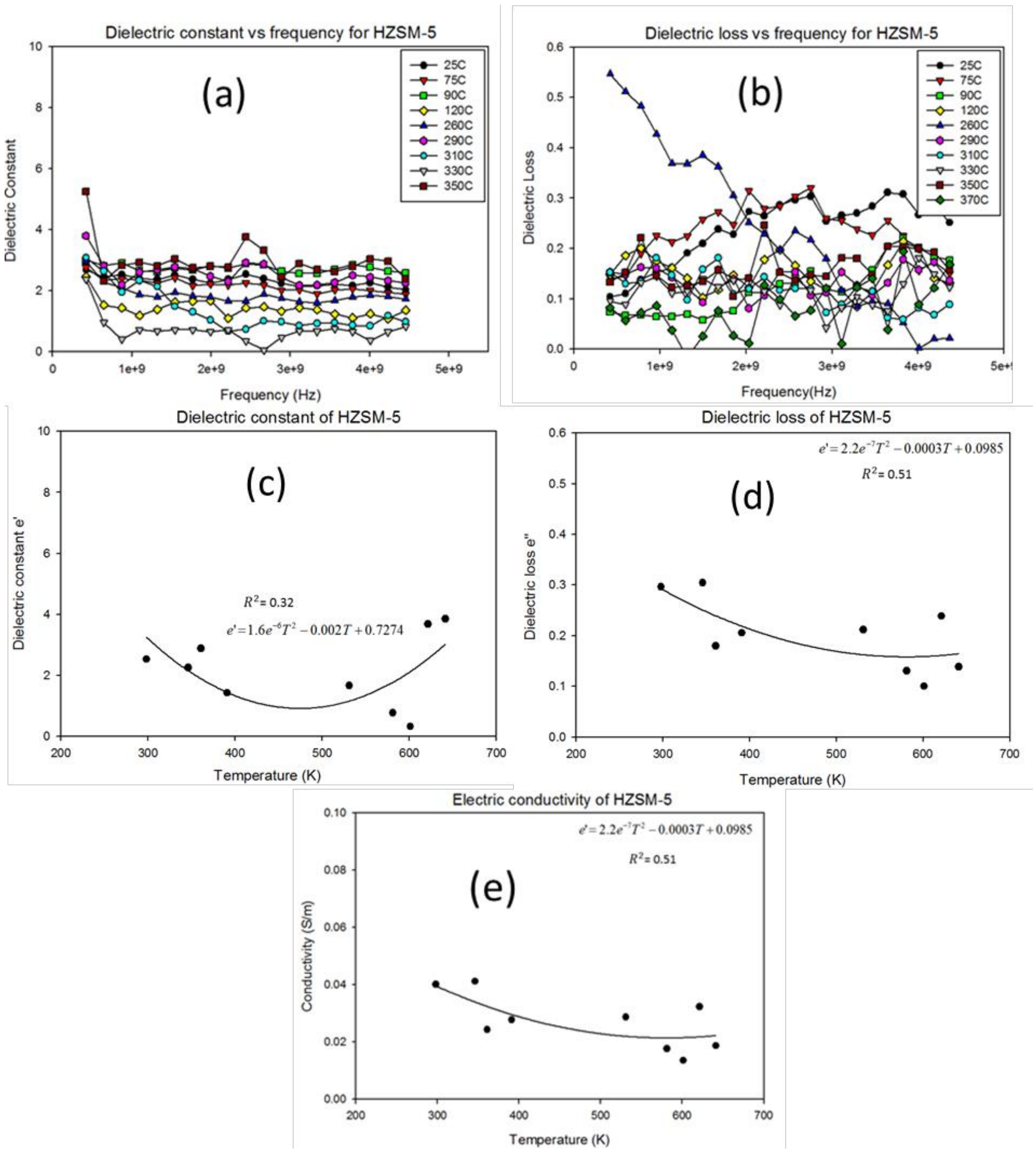

Figure 4 Dielectric properties of HZSM-5 powder at (a) different temperatures and (b) frequencies. (c) Electric conductivity, (d) dielectric loss and (e) dielectric constant of HZSM-5 at *2450 MHz* frequency at varying temperatures

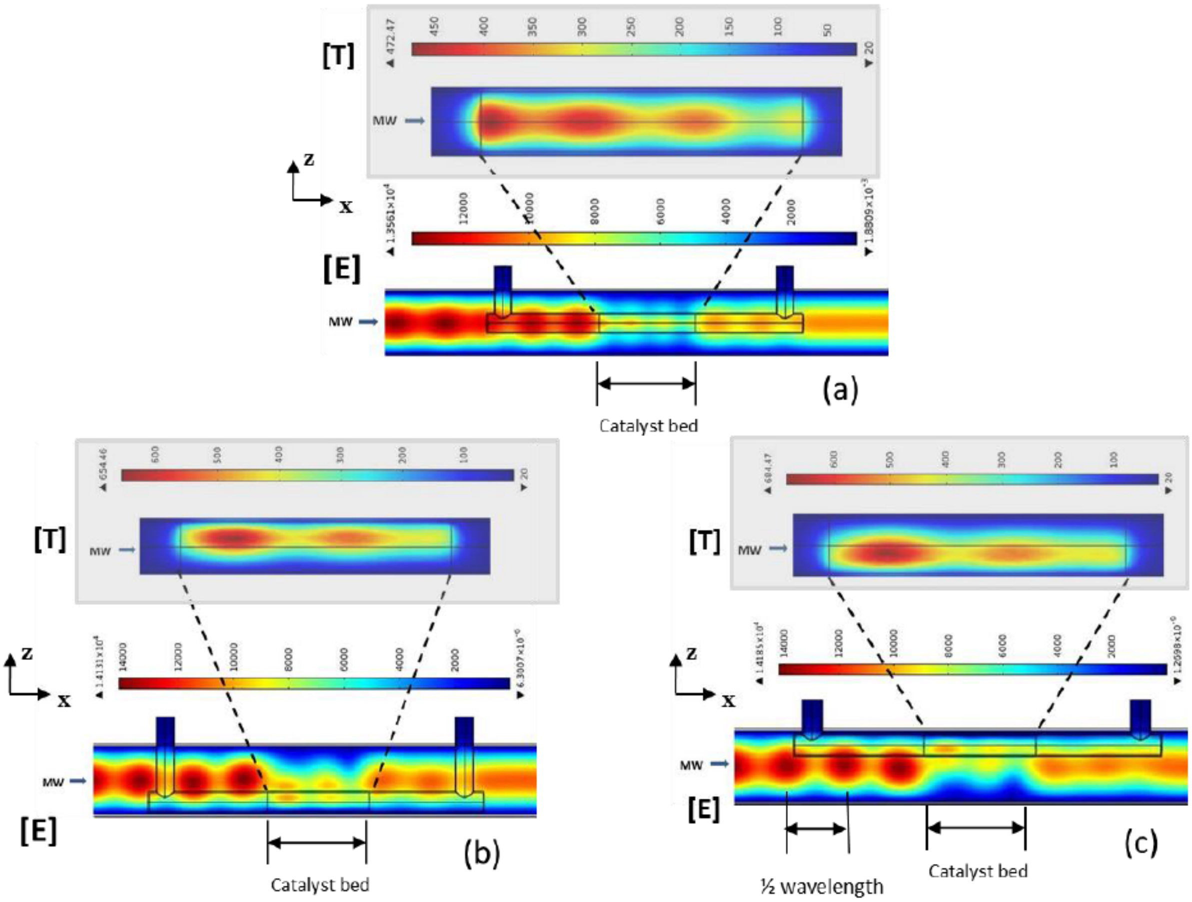

Figure 5 Electric field (V/m) and temperature profile for catalyst bed at (a) the center of the cavity *(z =0), (b)* the base of the cavity *(z =-0.03), (c)* the top of the cavity (*z =0.03*) (Note: different temperature scales)

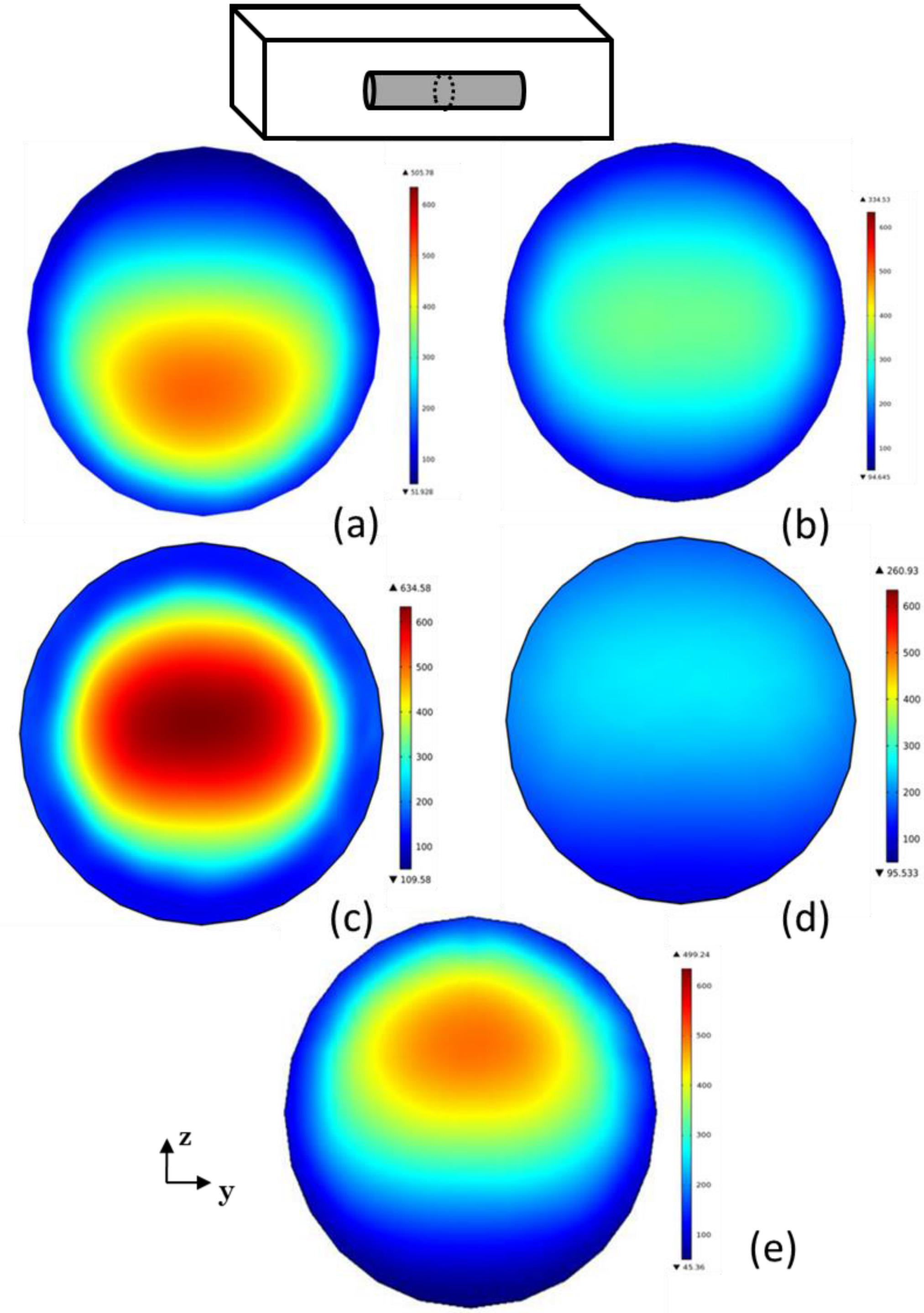

Figure 6 Temperature profile in *YZ*-direction at the center of the catalyst bed. The catalyst bed position is a) top of the waveguide $z=0.03\ m$, b) center of the waveguide $z=0$, c) $10\ mm$ off from the center $z = -0.01\ m$, d) $20\ mm$ off from the center of the waveguide $z = -0.02\ m$ and, e) base of the waveguide $z=-0.03\ m$. (Note: different temperature scales)

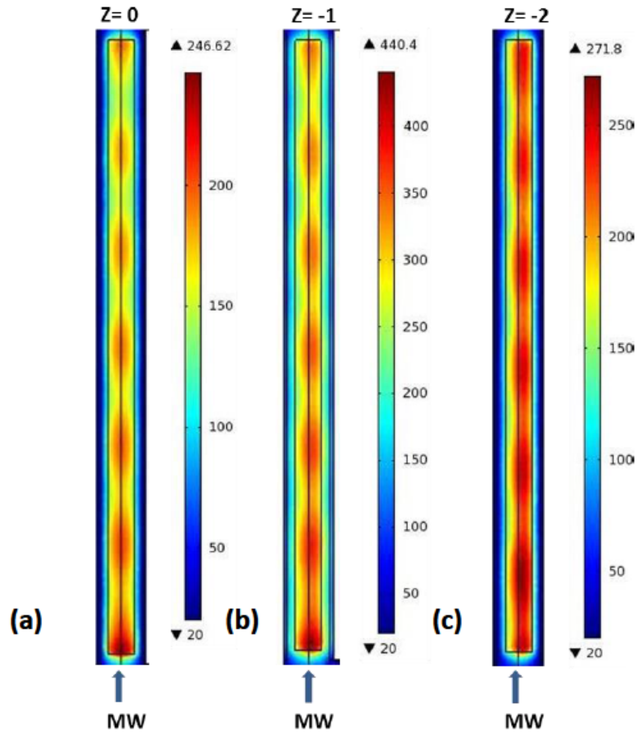

Figure 7 Temperature profile for narrow catalyst bed at different positions a) center ($z=0$), b) *10 mm* away from center ($z=-0.01$) and c) *20 mm* away from center ($z=-0.02$) (Note: different temperature scales)

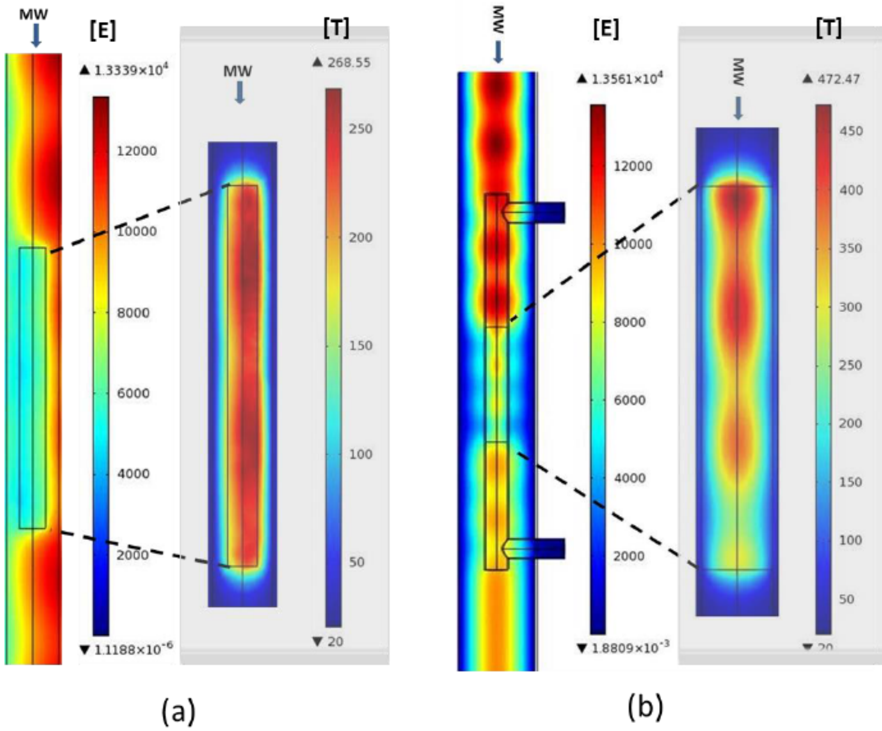

Figure 8 Electric field (*V/m*) and temperature (*℃*) in a) brick shaped catalyst bed and, b) cylindrical catalyst bed both placed in the center of the cavity (Note: different temperature scales)

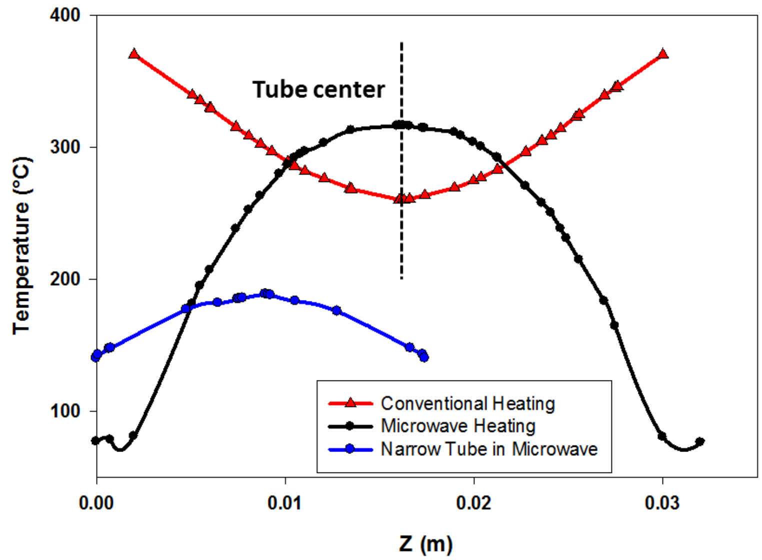

Figure 9 Temperature distribution along the centerline in z-axis (along the reactor tube radius) for microwave heating (regular sized and narrow catalyst bed) and conventional heating

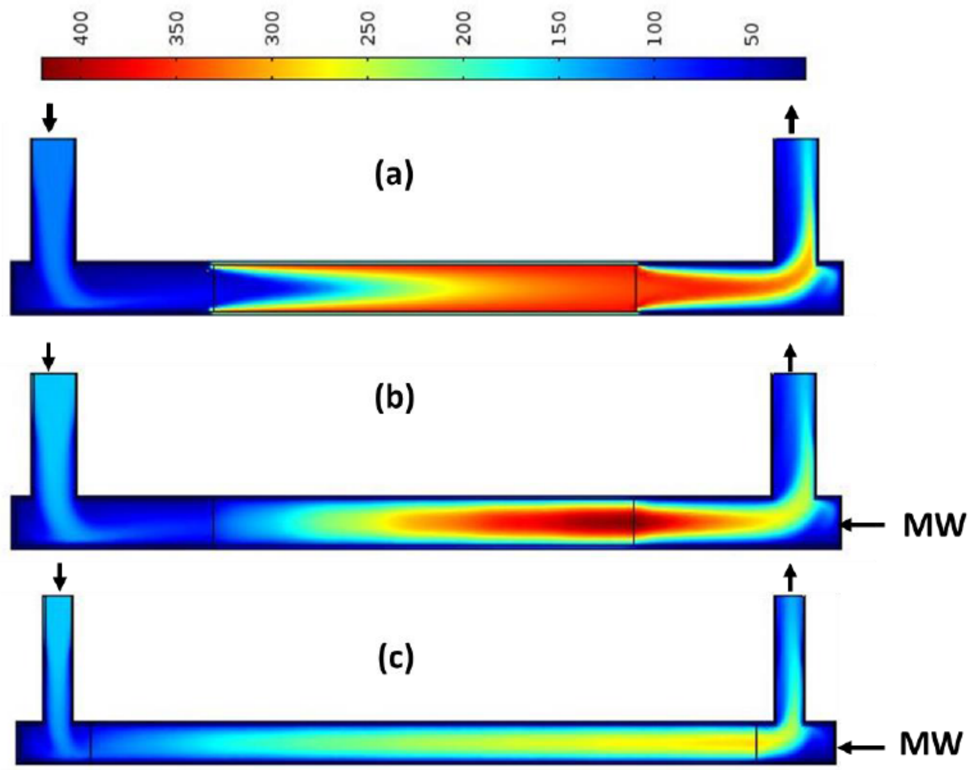

Figure 10 Longitudinal (*xz*-axis) temperature profile for (a) regular tube in conventional heating (b) regular tube in microwave (c) narrow tube in microwave

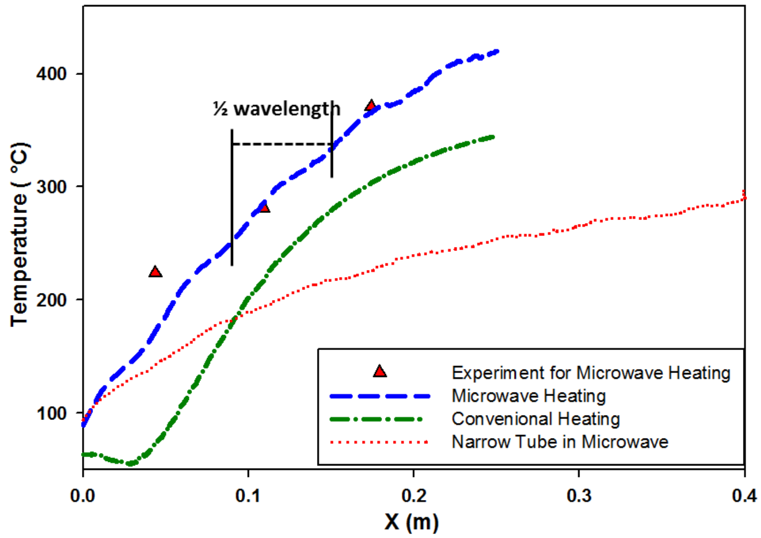

Figure 11 Temperature distribution along the centerline in *x*-axis for microwave heating (regular and narrow tube), conventional heating and experimental data (regular tube in microwave)

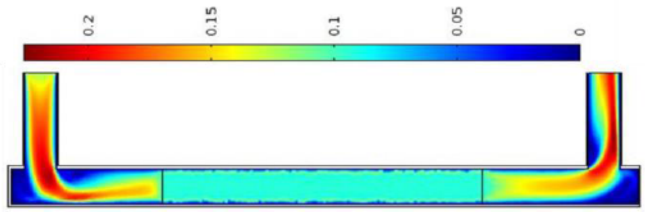

Figure 12 Velocity profile along the *zx*-axis